

Research Article

Multiple-Model Cardinality Balanced Multitarget Multi-Bernoulli Filter for Tracking Maneuvering Targets

Xianghui Yuan, Feng Lian, and Chongzhao Han

Ministry of Education Key Laboratory for Intelligent Networks and Network Security (MOE KLINNS),
School of Electronics and Information Engineering, Xi'an Jiaotong University, Xi'an 710049, China

Correspondence should be addressed to Feng Lian; lianfeng1981@mail.xjtu.edu.cn

Received 10 July 2013; Accepted 15 September 2013

Academic Editor: Xianxia Zhang

Copyright © 2013 Xianghui Yuan et al. This is an open access article distributed under the Creative Commons Attribution License, which permits unrestricted use, distribution, and reproduction in any medium, provided the original work is properly cited.

By integrating the cardinality balanced multitarget multi-Bernoulli (CBMeMber) filter with the interacting multiple models (IMM) algorithm, an MM-CBMeMber filter is proposed in this paper for tracking multiple maneuvering targets in clutter. The sequential Monte Carlo (SMC) method is used to implement the filter for generic multi-target models and the Gaussian mixture (GM) method is used to implement the filter for linear-Gaussian multi-target models. Then, the extended Kalman (EK) and unscented Kalman filtering approximations for the GM-MM-CBMeMber filter to accommodate mildly nonlinear models are described briefly. Simulation results are presented to show the effectiveness of the proposed filter.

1. Introduction

Recently, the random-finite-set-(RFS-) based multitarget tracking approaches [1] have attracted extensive attention. Although theoretically solid, the RFS-based approaches usually are involved with intractable computations. By introducing the finite-set statistics (FISST) [2], Mahler developed the probability hypothesis density (PHD) [3] and cardinalized PHD (CPHD) [4] filters, which have been shown to be a computationally tractable alternative to full multitarget Bayes filters in the RFS framework. The sequential Monte Carlo (SMC) implementations for the PHD and CPHD filters were devised by Zajic and Mahler [5], Sidenbladh [6], and Vo et al. [7]. Vo et al. and Zhang et al. [8–10] devised the Gaussian mixture (GM) implementations for the PHD and CPHD filters under the linear-Gaussian assumption on target dynamics, birth process, and sensor model. The PHD-based approaches have been successfully used for many real-world problems [11–13]. However, the SMC-PHD and SMC-CPHD approaches require clustering to extract state estimates from the particle population, which is expensive and unreliable [14, 15].

In 2007, Mahler proposed the multitarget multi-Bernoulli (MeMber) [2] recursion, which is an approximation to the full multitarget Bayes recursion using multi-Bernoulli RFSs

under low clutter density scenarios. In 2009, Vo et al. showed that the MeMber filter overestimates the number of targets and proposed a cardinality-balanced MeMber (CBMeMber) filter [16] to reduce the cardinality bias. Then, the SMC and GM implementations for the MeMber and CBMeMber filters were, respectively, proposed for generic and linear-Gaussian dynamic and measurement models. The MeMber and CBMeMber recursions propagate not the moments and cardinality distributions which are propagated by the PHD and CPHD filters but rather the approximate multitarget multi-Bernoulli posterior density. Therefore, the key advantage of the SMC-CBMeMber filter over the SMC-PHD and SMC-CPHD filters is that the multi-Bernoulli representation of the posterior density allows reliable and inexpensive extraction of state estimates. The CBMeMber filter has been applied for tracking multiple targets according to their audio and visual information [17].

The original CBMeMber filter does not consider the target maneuvers. Maneuvering targets might switch between different models of operation, so tracking using a single-model CBMeMber filter might fail since the filter does not match the actual system dynamics. It is well known that the interacting multiple models (IMM) approaches [18] have been proven to be very effective and have better performance

than the single-model filters in tracking a single maneuvering target without clutter. In the IMM approaches, a bank of filters, each matched with a different target motion model, operate in parallel. In general, there are three key steps in the IMM estimators: (1) mixing the model-conditioned estimates; (2) model-conditioned base-state estimation; (3) deriving the overall state estimate by combining the estimates from each model-conditioned base-state filters.

By integrating the CBMeMber filter with the IMM algorithm, an MM-CBMeMber filter is proposed to address the problem of tracking multiple maneuvering targets in clutter, which is much more difficult than the problem of tracking a single maneuvering target without clutter since the association between the measurements and the targets is unknown. The SMC method is used to implement the filter for generic multitarget models while the GM method is used to implement the filter for linear-Gaussian multitarget models. Then, the extended Kalman (EK) [19] and unscented Kalman (UK) [20] filtering approximations for the GM-MM-CBMeMber filter to accommodate mildly nonlinear models are described briefly. Nonlinear and linear-Gaussian examples of multiple maneuvering targets tracking are, respectively, presented for comparing the performance of the MM-CBMeMber filter with that of the single-model CBMeMber filters, MM-PHD filter [21–24], and MM-CPHD filter [25]. The simulation results show that (1) the proposed filter can estimate the number and states of multiple maneuvering targets effectively, whereas the performance of the single-model CBMeMber filters is rather poor; (2) under relatively low clutter density, the SMC-MM-CBMeMber filter outperforms the SMC-MM-PHD and SMC-MM-CPHD filters; (3) the performance of the GM-MM-CBMeMber filter is similar to that of the GM-MM-PHD filter and hence is inferior to that of GM-MM-CPHD filter.

The rest of the paper is organized as follows. Section 2 describes the problem of multiple maneuvering targets tracking. In Section 3, the MM-CBMeMber recursion is given. The generic SMC implementation of the MM-CBMeMber filter is described in Section 4. The analytic GM implementation of the MM-CBMeMber filter for linear-Gaussian multitarget models and its EK and UK extensions for nonlinear multitarget models are, respectively, given in Section 5. Numerical studies are shown in Section 6. The conclusions and the future work are given in Section 7.

2. Problem Statement for Multiple Maneuvering Targets Tracking

The multiple maneuvering targets appear and disappear randomly against time over an observation region. At time k , let $\mathbf{x}_k \in \mathbb{R}^n$ denote the kinematical state of a target and $n_k \in \mathbb{N}$ the label of the model in effect, where \mathbb{N} is the discrete set of all model labels. The models follow a discrete Markov chain with transition probability $h_{k|k-1}(n_k | n_{k-1})$. Let $\mathbf{y}_k = (\mathbf{x}_k, n_k) \in \mathbb{R}^n \times \mathbb{N}$ denote the augmented state vector, whose transition is governed by the density

$$f_{k|k-1}(\mathbf{y}_k | \mathbf{y}_{k-1}) = f_{k|k-1}(\mathbf{x}_k | \mathbf{x}_{k-1}, n_k) h_{k|k-1}(n_k | n_{k-1}), \quad (1)$$

where $f_{k|k-1}(\mathbf{x}_k | \mathbf{x}_{k-1}, n_k)$ is the kinematical state transition density conditioned on model n_k .

The measurement originates either from target or from random clutter (false alarm). Moreover, the target-generated measurements are indistinguishable from the clutter. At time k , let $\mathbf{z}_k \in \mathbb{R}^m$ denote the measurement vector received by a sensor. The single-measurement single-target likelihood is described by the density conditioned on model n_k

$$g_k(\mathbf{z}_k | \mathbf{y}_k) = f_{k|k}(\mathbf{z}_k | \mathbf{x}_k, n_k). \quad (2)$$

At time k , let T_k denote the number of the existing targets and S_k the number of the measurements. Then, multiple augmented states and unlabelled sensor measurements can be represented as finite sets $Y_k = \{(\mathbf{x}_k^{(i)}, n_k^{(i)})\}_{i=1}^{T_k}$ and $Z_k = \{\mathbf{z}_k^{(s)}\}_{s=1}^{S_k}$, respectively. In addition, let $Z_{1:k} \triangleq Z_1, \dots, Z_k$ denote a sequence of the measurement sets available up to and including time k .

3. MM-CBMeMber Filter

A Bernoulli RFS Y_k has probability $1 - r_k$ of being empty and probability r_k ($0 \leq r_k \leq 1$) of being a singleton whose only element is distributed according to a probability density p_k . The probability density of Y_k is

$$\pi(Y_k) = \begin{cases} 1 - r_k, & Y_k = \emptyset, \\ r_k p_k(\mathbf{x}_k, n_k), & Y_k = \{(\mathbf{x}_k, n_k)\}. \end{cases} \quad (3)$$

A multi-Bernoulli RFS Y_k is a union of a fixed number of independent Bernoulli RFSs $Y_k^{(i)}$, $i = 1, \dots, M_k$, that is, $Y_k = \bigcup_{i=1}^{M_k} Y_k^{(i)}$. Y_k is thus completely described by the multi-Bernoulli parameter set $\{(r_k^{(i)}, p_k^{(i)}(\mathbf{x}_k, n_k))\}_{i=1}^{M_k}$ with the mean cardinality $\sum_{i=1}^{M_k} r_k^{(i)}$ and the probability density [2]

$$\pi(Y_k) = \prod_{j=1}^{M_k} (1 - r_k^{(j)}) \sum_{1 \leq i_1 \neq \dots \neq i_{|Y_k|} \leq M_k} \prod_{j=1}^{|Y_k|} \frac{r_k^{(i_j)} p_k^{(i_j)}(\mathbf{x}_k, n_k)}{1 - r_k^{(i_j)}}, \quad (4)$$

where $|\cdot|$ denotes the cardinality of a set.

Throughout this paper, we abbreviate a probability density of the form (4) by $\pi(Y_k) = \{(r_k^{(i)}, p_k^{(i)}(\mathbf{x}_k, n_k))\}_{i=1}^{M_k}$.

Let $p_{S,k}(\mathbf{y}_{k-1})$ denote the probability that the maneuvering target with augmented state \mathbf{y}_{k-1} survives at time k ; let $p_{D,k}(\mathbf{y}_k)$ denote the probability that the maneuvering target with augmented state \mathbf{y}_k generates an observation at time k . RFS modeling the multiple maneuvering targets state Y_k and the sensor measurement Z_k are, respectively, given by the union

$$Y_k = \left[\bigcup_{\mathbf{y}_{k-1} \in Y_{k-1}} \Omega_{k|k-1}(\mathbf{y}_{k-1}) \right] \cup \Gamma_k, \quad (5)$$

$$Z_k = \left[\bigcup_{\mathbf{y}_k \in Y_k} \Theta_k(\mathbf{y}_k) \right] \cup K_k,$$

where Γ_k denotes the multi-Bernoulli RFS of spontaneous births; the Bernoulli RFS $\Omega_{k|k-1}(\mathbf{y}_{k-1})$ with $r_k = p_{S,k}(\mathbf{y}_{k-1})$ and $p_k(\mathbf{y}_k) = f_{k|k-1}(\mathbf{y}_k | \mathbf{y}_{k-1})$ is used to model the dynamic behavior of $\mathbf{y}_{k-1} \in Y_{k-1}$; the Bernoulli RFS $\Theta_k(\mathbf{y}_k)$ with $r_k = p_{D,k}(\mathbf{y}_k)$ and $p_k(\mathbf{z}_k) = g_k(\mathbf{z}_k | \mathbf{y}_k)$ is used to model the observation behavior of $\mathbf{y}_k \in Y_k$; the clutter is modeled as a Poisson RFS K_k with the intensity $\kappa_k(\mathbf{z}_k) = \lambda_{c,k} f_{c,k}(\mathbf{z}_k)$, where $\lambda_{c,k}$ and $f_{c,k}(\cdot)$ are, respectively, the average clutter number and the probability density of clutter spatial distribution at time k .

Based on the above RFS models of the multiple maneuvering targets and the method of Mahler's FISST, the MM-CBMeMber filter, which implicitly requires a finite number of single-model CBMeMber filters operate in parallel, is derived by introducing the mixing and combination strategies in the IMM approaches [18]. As the multiple-model approaches, the MM-CBMeMber filter does not need a maneuver detection decision and undergoes a soft switching between the models. One cycle of the recursive MM-CBMeMber algorithm can be described as follows.

(1) *The Mixing and Prediction Stage.* If at time $k-1$, the posterior density is a multi-Bernoulli of the form $\pi_{k-1}(Y_{k-1} | Z_{1:k-1}) = \{(r_{k-1}^{(i)}, p_{k-1}^{(i)}(\mathbf{x}_{k-1}, n_{k-1}))\}_{i=1}^{M_{k-1}}$, then the mixed multi-Bernoulli density is

$$\widehat{\pi}_{k-1}(\widehat{Y}_{k-1} | Z_{1:k-1}) = \{(r_{k-1}^{(i)}, p_{k-1}^{(i)}(\mathbf{x}_{k-1}, n_k))\}_{i=1}^{M_{k-1}}, \quad (6)$$

where

$$\begin{aligned} p_{k-1}^{(i)}(\mathbf{x}_{k-1}, n_k) &= \sum_{n_{k-1}} p_{k-1}^{(i)}(\mathbf{x}_{k-1}, n_k, n_{k-1}) \\ &= \sum_{n_{k-1}} p_{k-1}^{(i)}(n_k | \mathbf{x}_{k-1}, n_{k-1}) p_{k-1}^{(i)}(\mathbf{x}_{k-1}, n_{k-1}). \end{aligned} \quad (7)$$

Since the models switching is only decided by the model transition probability and is independent of the target kinematical state:

$$= \sum_{n_{k-1}} h_{k|k-1}(n_k | n_{k-1}) p_{k-1}^{(i)}(\mathbf{x}_{k-1}, n_{k-1}) \quad (8)$$

is a combination of the previous model-dependent densities. Finally, the mixed and predicted density is also a multi-Bernoulli and is given by

$$\begin{aligned} \pi_{k|k-1}(Y_k | Z_{1:k-1}) &= \{(r_{P,k|k-1}^{(i)}, p_{P,k|k-1}^{(i)}(\mathbf{x}_k, n_k))\}_{i=1}^{M_{k-1}} \\ &\cup \{(r_{\Gamma,k}^{(i)}, p_{\Gamma,k}^{(i)}(\mathbf{x}_k, n_k))\}_{i=1}^{M_{\Gamma,k}}, \end{aligned} \quad (9)$$

where $\{(r_{\Gamma,k}^{(i)}, p_{\Gamma,k}^{(i)}(\mathbf{x}_k, n_k))\}_{i=1}^{M_{\Gamma,k}}$ are the parameters of the multi-Bernoulli RFS of births at time k :

$$\begin{aligned} r_{P,k|k-1}^{(i)} &= r_{k-1}^{(i)} \sum_{n_k} \sum_{n_{k-1}} h_{k|k-1}(n_k | n_{k-1}) \\ &\quad \times \langle p_{k-1}^{(i)}(\cdot, n_{k-1}), p_{S,k}(\cdot, n_{k-1}) \rangle, \\ p_{P,k|k-1}^{(i)}(\mathbf{x}_k, n_k) &= \left(\sum_{n_{k-1}} h_{k|k-1}(n_k | n_{k-1}) \right. \\ &\quad \times \langle f_{k|k-1}(\mathbf{x}_k | \cdot, n_k), p_{k-1}^{(i)}(\cdot, n_{k-1}) p_{S,k}(\cdot, n_{k-1}) \rangle \left. \right) \\ &\quad \times \left(\sum_{n_k} \sum_{n_{k-1}} h_{k|k-1}(n_k | n_{k-1}) \right. \\ &\quad \times \langle p_{k-1}^{(i)}(\cdot, n_{k-1}), p_{S,k}(\cdot, n_{k-1}) \rangle \left. \right)^{-1}, \end{aligned} \quad (10)$$

where $\langle \cdot, \cdot \rangle$ defines the integral inner product, that is,

$$\begin{aligned} &\langle p_{k-1}^{(i)}(\cdot, n_{k-1}), p_{S,k}(\cdot, n_{k-1}) \rangle \\ &= \int p_{k-1}^{(i)}(\mathbf{x}_{k-1}, n_{k-1}) p_{S,k}(\mathbf{x}_{k-1}, n_{k-1}) d\mathbf{x}_{k-1}. \end{aligned} \quad (11)$$

(2) *The Update Stage.* If at time k , the mixed and predicted density is a multi-Bernoulli of the form $\pi_{k|k-1}(Y_k | Z_{1:k-1}) = \{(r_{k|k-1}^{(i)}, p_{k|k-1}^{(i)}(\mathbf{x}_k, n_k))\}_{i=1}^{M_{k|k-1}}$, then the posterior density can be approximated by a multi-Bernoulli as follows:

$$\begin{aligned} \pi_k(Y_k | Z_k) &\approx \{(r_{L,k}^{(i)}, p_{L,k}^{(i)}(\mathbf{x}_k, n_k))\}_{i=1}^{M_{k|k-1}} \\ &\cup \{(r_{U,k}(\mathbf{z}_k), p_{U,k}(\mathbf{x}_k, n_k; \mathbf{z}_k))\}_{\mathbf{z}_k \in Z_k}, \end{aligned} \quad (12)$$

where

$$r_{L,k}^{(i)} = r_{k|k-1}^{(i)} \frac{1 - \sum_{n_k} \langle p_{k|k-1}^{(i)}(\cdot, n_k), p_{D,k}(\cdot, n_k) \rangle}{1 - r_{k|k-1}^{(i)} \sum_{n_k} \langle p_{k|k-1}^{(i)}(\cdot, n_k), p_{D,k}(\cdot, n_k) \rangle},$$

$$\begin{aligned}
p_{L,k}^{(i)}(\mathbf{x}_k, n_k) &= \frac{(1 - p_{D,k}(\mathbf{x}_k, n_k)) p_{k|k-1}^{(i)}(\mathbf{x}_k, n_k)}{1 - \sum_{n_k} \langle p_{k|k-1}^{(i)}(\cdot, n_k), p_{D,k}(\cdot, n_k) \rangle}, \\
r_{U,k}(\mathbf{z}_k) &= \left(\sum_{i=1}^{M_{k|k-1}} \frac{(1 - r_{k|k-1}^{(i)}) r_{k|k-1}^{(i)} \sum_{n_k} \langle p_{k|k-1}^{(i)}(\cdot, n_k), g_k(\mathbf{z}_k | \cdot, n_k) p_{D,k}(\cdot, n_k) \rangle}{(1 - r_{k|k-1}^{(i)} \sum_{n_k} \langle p_{k|k-1}^{(i)}(\cdot, n_k), p_{D,k}(\cdot, n_k) \rangle)^2} \right) \\
&\quad \times \left(\kappa_k(\mathbf{z}_k) + \sum_{i=1}^{M_{k|k-1}} \frac{r_{k|k-1}^{(i)} \sum_{n_k} \langle p_{k|k-1}^{(i)}(\cdot, n_k), g_k(\mathbf{z}_k | \cdot, n_k) p_{D,k}(\cdot, n_k) \rangle}{1 - r_{k|k-1}^{(i)} \sum_{n_k} \langle p_{k|k-1}^{(i)}(\cdot, n_k), p_{D,k}(\cdot, n_k) \rangle} \right)^{-1}, \\
p_{U,k}(\mathbf{x}_k, n_k; \mathbf{z}_k) &= \frac{\sum_{i=1}^{M_{k|k-1}} (r_{k|k-1}^{(i)} / (1 - r_{k|k-1}^{(i)})) p_{k|k-1}^{(i)}(\mathbf{x}_k, n_k) g_k(\mathbf{z}_k | \mathbf{x}_k, n_k) p_{D,k}(\mathbf{x}_k, n_k)}{\sum_{i=1}^{M_{k|k-1}} (r_{k|k-1}^{(i)} / (1 - r_{k|k-1}^{(i)})) \sum_{n_k} \langle p_{k|k-1}^{(i)}(\cdot, n_k), g_k(\mathbf{z}_k | \cdot, n_k) p_{D,k}(\cdot, n_k) \rangle}.
\end{aligned} \tag{13}$$

(3) *The Multitarget State Estimation.* For the multi-Bernoulli representation $\pi_k(Y_k | Z_k) = \{(r_k^{(i)}, p_k^{(i)}(\mathbf{x}_k, n_k))\}_{i=1}^{M_k}$, the extraction of multitarget number and state estimates are straightforward since the probability $r_k^{(i)}$ indicates how likely the i th hypothesized track is a true track, and the posterior density $p_k^{(i)}(\mathbf{x}_k, n_k)$ describes the distribution of the estimated augmented state of the track. The state estimation procedure for the MM-CBMeMber filter [8] is summarized in Algorithm 1.

4. SMC-MM-CBMeMber Filter

In this section, a generic SMC implementation of the proposed MM-CBMeMber filter is presented for accommodating nonlinear dynamic and measurement models. In this implementation, the samples or particles, which are used to represent the multi-Bernoulli density of multiple maneuvering targets, consists of the kinematical state and model information with associated weights. One cycle of the recursive SMC-MM-CBMeMber algorithm can be described as follows.

(1) *The SMC Mixing and Prediction Stage.* Suppose that at time $k-1$ the multi-Bernoulli posterior density $\tilde{\pi}_{k-1}(Y_{k-1} | Z_{1:k-1}) = \{(\tilde{r}_{k-1}^{(i)}, \tilde{p}_{k-1}^{(i)}(\mathbf{x}_{k-1}, n_{k-1}))\}_{i=1}^{M_{k-1}}$ is given and each $\tilde{p}_{k-1}^{(i)}(\mathbf{x}_{k-1}, n_{k-1})$, $i = 1, \dots, M_{k-1}$, is composed of a set of weighted samples $\{\omega_{k-1}^{(i,l)}, \mathbf{x}_{k-1}^{(i,l)}, n_{k-1}^{(i,l)}\}_{l=1}^{L_{k-1}^{(i)}}$,

$$\tilde{p}_{k-1}^{(i)}(\mathbf{x}_{k-1}, n_{k-1}) = \sum_{l=1}^{L_{k-1}^{(i)}} \omega_{k-1}^{(i,l)} \delta(\mathbf{x}_{k-1} - \mathbf{x}_{k-1}^{(i,l)}, n_{k-1} - n_{k-1}^{(i,l)}), \tag{14}$$

where $\delta(\mathbf{x} - \mathbf{x}^{(c)})$ is Dirac delta function centered at $\mathbf{x}^{(c)}$. Then, the mixed and predicted multi-Bernoulli density $\tilde{\pi}_{k|k-1}(Y_k | Z_{1:k-1}) = \{(\tilde{r}_{k|k-1}^{(i)}, \tilde{p}_{k|k-1}^{(i)}(\mathbf{x}_k, n_k))\}_{i=1}^{M_{k-1}} \cup \{(\tilde{r}_{\Gamma,k}^{(i)}, \tilde{p}_{\Gamma,k}^{(i)}(\mathbf{x}_k, n_k))\}_{i=1}^{M_{\Gamma,k}}$ can be computed as follows:

$$\begin{aligned}
\tilde{r}_{P,k|k-1}^{(i)} &= \tilde{r}_{k-1}^{(i)} \sum_{l=1}^{L_{k-1}^{(i)}} \omega_{k-1}^{(i,l)} p_{S,k}(\mathbf{x}_{k-1}^{(i,l)}, n_{k-1}^{(i,l)}) \frac{h_{k|k-1}(n_{P,k|k-1}^{(i,l)} | n_{k-1}^{(i,l)})}{\alpha_k^{(i)}(n_{P,k|k-1}^{(i,l)} | n_{k-1}^{(i,l)})}, \\
\tilde{r}_{\Gamma,k}^{(i)} &= \text{parameter given by birth model}, \\
\tilde{p}_{P,k|k-1}^{(i)}(\mathbf{x}_k, n_k) &= \sum_{l=1}^{L_{k-1}^{(i)}} \omega_{P,k|k-1}^{(i,l)} \delta(\mathbf{x}_k - \mathbf{x}_{P,k|k-1}^{(i,l)}, n_k - n_{P,k|k-1}^{(i,l)}), \\
\tilde{p}_{\Gamma,k}^{(i)}(\mathbf{x}_k, n_k) &= \sum_{l=1}^{L_{\Gamma,k}^{(i)}} \omega_{\Gamma,k}^{(i,l)} \delta(\mathbf{x}_k - \mathbf{x}_{\Gamma,k}^{(i,l)}, n_k - n_{\Gamma,k}^{(i,l)}),
\end{aligned} \tag{15}$$

where the particles $\mathbf{x}_{P,k|k-1}^{(i,l)}, n_{P,k|k-1}^{(i,l)}$ corresponding to the surviving maneuvering targets can be derived by sampling from the proposal densities $q_k^{(i)}(\cdot | \mathbf{x}_{k-1}, n_k, Z_k)$ and $\alpha_k^{(i)}(\cdot | n_{k-1})$

$$\begin{aligned}
n_{P,k|k-1}^{(i,l)} &\sim \alpha_k^{(i)}(\cdot | n_{k-1}^{(i,l)}) \\
\mathbf{x}_{P,k|k-1}^{(i,l)} &\sim q_k^{(i)}(\cdot | \mathbf{x}_{k-1}^{(i,l)}, n_{P,k|k-1}^{(i,l)}, Z_k) \quad l = 1, \dots, L_{k-1}^{(i)}
\end{aligned} \tag{16}$$

with the associated weights

$$\begin{aligned}
\omega_{P,k|k-1}^{(i,l)} &= \frac{\tilde{\omega}_{P,k|k-1}^{(i,l)}}{\sum_{l=1}^{L_{k-1}^{(i)}} \tilde{\omega}_{P,k|k-1}^{(i,l)}}, \\
\tilde{\omega}_{P,k|k-1}^{(i,l)} &= \frac{f_{k|k-1}(\mathbf{x}_{P,k|k-1}^{(i,l)} | \mathbf{x}_{k-1}^{(i,l)}, n_{P,k|k-1}^{(i,l)}) p_{S,k}(\mathbf{x}_{k-1}^{(i,l)}, n_{k-1}^{(i,l)})}{q_k^{(i)}(\mathbf{x}_{P,k|k-1}^{(i,l)} | \mathbf{x}_{k-1}^{(i,l)}, n_{P,k|k-1}^{(i,l)}, Z_k)} \\
&\quad \cdot \frac{h_{k|k-1}(n_{P,k|k-1}^{(i,l)} | n_{k-1}^{(i,l)})}{\alpha_k^{(i)}(n_{P,k|k-1}^{(i,l)} | n_{k-1}^{(i,l)})} \cdot \omega_{k-1}^{(i,l)}
\end{aligned} \tag{17}$$

and the particles $\mathbf{x}_{\Gamma,k}^{(i,l)}, n_{\Gamma,k}^{(i,l)}$ corresponding to the new born maneuvering targets can be derived by sampling from the proposal densities $b_k^{(i)}(\cdot | n_k, Z_k)$ and $\beta_k^{(i)}(\cdot)$

$$\begin{aligned}
n_{\Gamma,k}^{(i,l)} &\sim \beta_k^{(i)}(\cdot) \\
\mathbf{x}_{\Gamma,k}^{(i,l)} &\sim b_k^{(i)}(\cdot | n_{\Gamma,k}^{(i,l)}, Z_k) \quad l = 1, \dots, L_{\Gamma,k}^{(i)}
\end{aligned} \tag{18}$$

given $\pi_k(Y_k | Z_k) = \{(r_k^{(i)}, p_k^{(i)}(\mathbf{x}_k, n_k))\}_{i=1}^{M_k}$; set $\widehat{T}_k = 0, \widehat{X}_k = \emptyset$
for $i = 1, \dots, M_k$,
if $r_k^{(i)} > \text{a given threshold (i.e. 0.5)}$;
 $\widehat{T}_k = \widehat{T}_k + 1$,
 $\widehat{\mathbf{x}}_k^{(\widehat{T}_k)} = \sum_{n_k} \overbrace{p_k^{(i)}(n_k)}^{\text{probability of model } n_k} \cdot \overbrace{\int \mathbf{x}_k p_k^{(i)}(\mathbf{x}_k | n_k) d\mathbf{x}_k}^{\text{state estimation conditioned on model } n_k} = \sum_{n_k} \int \mathbf{x}_k p_k^{(i)}(\mathbf{x}_k, n_k) d\mathbf{x}_k$,
 $\widehat{X}_k := [\widehat{X}_k, \widehat{\mathbf{x}}_k^{(\widehat{T}_k)}]$;
end;
end;
output: $\widehat{X}_k = \{\widehat{\mathbf{x}}_k^{(i)}\}_{i=1}^{\widehat{T}_k}$

ALGORITHM 1: Multitarget state estimation procedure for the MM-CBMeMber filter.

with the associated weights

$$\omega_{\Gamma,k}^{(i,l)} = \frac{\tilde{\omega}_{\Gamma,k}^{(i,l)}}{\sum_{l=1}^{L_{\Gamma,k}^{(i)}} \tilde{\omega}_{\Gamma,k}^{(i,l)}}, \quad (19)$$

$$\tilde{\omega}_{\Gamma,k}^{(i,l)} = \frac{p_{\Gamma,k}^{(i)}(\mathbf{x}_{\Gamma,k}^{(i,l)}, n_{\Gamma,k}^{(i,l)})}{b_k^{(i)}(\mathbf{x}_{\Gamma,k}^{(i,l)} | n_{\Gamma,k}^{(i,l)}, Z_k) \beta_k^{(i)}(n_{\Gamma,k}^{(i,l)})}.$$

(2) *The SMC Update Stage.* Suppose that at time k the mixed and predicted multi-Bernoulli density $\tilde{\pi}_{k|k-1}(Y_k | Z_{1:k-1}) =$

$\{(\tilde{r}_{k|k-1}^{(i)}, \tilde{p}_{k|k-1}^{(i)}(\mathbf{x}_k, n_k))\}_{i=1}^{M_{k|k-1}}$ is given and each $\tilde{p}_{k|k-1}^{(i)}(\mathbf{x}_k, n_k)$, $i = 1, \dots, M_{k|k-1}$, is composed of a set of weighted samples $\{\omega_{k|k-1}^{(i,l)}, \mathbf{x}_{k|k-1}^{(i,l)}, n_{k|k-1}^{(i,l)}\}_{l=1}^{L_{k|k-1}^{(i)}}$,

$$\tilde{p}_{k|k-1}^{(i)}(\mathbf{x}_k, n_k) = \sum_{l=1}^{L_{k|k-1}^{(i)}} \omega_{k|k-1}^{(i,l)} \delta(\mathbf{x}_k - \mathbf{x}_{k|k-1}^{(i,l)}, n_k - n_{k|k-1}^{(i,l)}). \quad (20)$$

Then, the multi-Bernoulli approximation of the updated density $\tilde{\pi}_k(Y_k | Z_{1:k}) \approx \{(\tilde{r}_{L,k}^{(i)}, \tilde{p}_{L,k}^{(i)}(\mathbf{x}_k, n_k))\}_{i=1}^{M_{k|k-1}} \cup \{(\tilde{r}_{U,k}(\mathbf{z}_k), \tilde{p}_{U,k}(\mathbf{x}_k, n_k; \mathbf{z}_k))\}_{\mathbf{z}_k \in Z_k}$ can be computed as follows:

$$\tilde{r}_{L,k}^{(i)} = \tilde{r}_{k|k-1}^{(i)} \frac{1 - \sum_{l=1}^{L_{k|k-1}^{(i)}} \omega_{k|k-1}^{(i,l)} p_{D,k}(\mathbf{x}_{k|k-1}^{(i,l)}, n_{k|k-1}^{(i,l)})}{1 - \tilde{r}_{k|k-1}^{(i)} \sum_{l=1}^{L_{k|k-1}^{(i)}} \omega_{k|k-1}^{(i,l)} p_{D,k}(\mathbf{x}_{k|k-1}^{(i,l)}, n_{k|k-1}^{(i,l)})},$$

$$\tilde{p}_{L,k}^{(i)}(\mathbf{x}_k, n_k) = \sum_{l=1}^{L_{k|k-1}^{(i)}} \omega_{L,k}^{(i,l)} \delta(\mathbf{x}_k - \mathbf{x}_{k|k-1}^{(i,l)}, n_k - n_{k|k-1}^{(i,l)}),$$

$$\tilde{r}_{U,k}(\mathbf{z}_k) = \left(\sum_{i=1}^{M_{k|k-1}} \frac{(1 - \tilde{r}_{k|k-1}^{(i)}) \tilde{r}_{k|k-1}^{(i)} \sum_{l=1}^{L_{k|k-1}^{(i)}} \omega_{k|k-1}^{(i,l)} g_k(\mathbf{z}_k | \mathbf{x}_{k|k-1}^{(i,l)}, n_{k|k-1}^{(i,l)}) p_{D,k}(\mathbf{x}_{k|k-1}^{(i,l)}, n_{k|k-1}^{(i,l)})}{\left(1 - \tilde{r}_{k|k-1}^{(i)} \sum_{l=1}^{L_{k|k-1}^{(i)}} \omega_{k|k-1}^{(i,l)} p_{D,k}(\mathbf{x}_{k|k-1}^{(i,l)}, n_{k|k-1}^{(i,l)})\right)^2} \right) \quad (21)$$

$$\times \left(\kappa_k(\mathbf{z}_k) + \sum_{i=1}^{M_{k|k-1}} \frac{\tilde{r}_{k|k-1}^{(i)} \sum_{l=1}^{L_{k|k-1}^{(i)}} \omega_{k|k-1}^{(i,l)} g_k(\mathbf{z}_k | \mathbf{x}_{k|k-1}^{(i,l)}, n_{k|k-1}^{(i,l)}) p_{D,k}(\mathbf{x}_{k|k-1}^{(i,l)}, n_{k|k-1}^{(i,l)})}{1 - \tilde{r}_{k|k-1}^{(i)} \sum_{l=1}^{L_{k|k-1}^{(i)}} \omega_{k|k-1}^{(i,l)} p_{D,k}(\mathbf{x}_{k|k-1}^{(i,l)}, n_{k|k-1}^{(i,l)})} \right)^{-1},$$

$$\tilde{p}_{U,k}(\mathbf{x}_k, n_k; \mathbf{z}_k) = \sum_{i=1}^{M_{k|k-1}} \sum_{l=1}^{L_{k|k-1}^{(i)}} \omega_{U,k}^{(i,l)}(\mathbf{z}_k) \delta(\mathbf{x}_k - \mathbf{x}_{k|k-1}^{(i,l)}, n_k - n_{k|k-1}^{(i,l)}),$$

where

$$\begin{aligned}\omega_{L,k}^{(i,l)} &= \frac{\tilde{\omega}_{L,k}^{(i,l)}}{\sum_{l=1}^{L_{k|k-1}^{(i)}} \tilde{\omega}_{L,k}^{(i,l)}}, \\ \tilde{\omega}_{L,k}^{(i,l)} &= \omega_{k|k-1}^{(i,l)} \frac{1 - P_{D,k}(\mathbf{x}_{k|k-1}, n_{k|k-1}^{(i,l)})}{1 - \sum_{l=1}^{L_{k|k-1}^{(i)}} \omega_{k|k-1}^{(i,l)} P_{D,k}(\mathbf{x}_{k|k-1}, n_{k|k-1}^{(i,l)})}, \\ \omega_{U,k}^{(i,l)}(\mathbf{z}_k) &= \frac{\tilde{\omega}_{U,k}^{(i,l)}(\mathbf{z}_k)}{\sum_{i=1}^{M_{k|k-1}} \sum_{l=1}^{L_{k|k-1}^{(i)}} \tilde{\omega}_{U,k}^{(i,l)}(\mathbf{z}_k)}, \\ \tilde{\omega}_{U,k}^{(i,l)}(\mathbf{z}_k) &= \frac{\tilde{r}_{k|k-1}^{(i)}}{1 - \tilde{r}_{k|k-1}^{(i)}} \omega_{k|k-1}^{(i,l)} g_k \\ &\quad \times (\mathbf{z}_k | \mathbf{x}_{k|k-1}, n_{k|k-1}^{(i,l)}) P_{D,k}(\mathbf{x}_{k|k-1}, n_{k|k-1}^{(i,l)}).\end{aligned}\quad (22)$$

(3) *The Resampling and Pruning Stage.* It is the same as the resampling and pruning stage of the SMC-CBMeMber filter [16].

(4) *The SMC Multitarget State Estimation.* Given the SMC multi-Bernoulli posterior density

$$\begin{aligned}\tilde{\pi}_k(Y_k | Z_{1:k}) &= \left\{ \left(\tilde{r}_k^{(i)}, \tilde{p}_k^{(i)}(\mathbf{x}_k, n_k) \right) \right\}_{i=1}^{M_k} \\ \text{with } \tilde{p}_k^{(i)}(\mathbf{x}_k, n_k) &= \sum_{l=1}^{L_k^{(i)}} \omega_k^{(i,l)} \delta(\mathbf{x}_k - \mathbf{x}_k^{(i,l)}, n_k - n_k^{(i,l)}),\end{aligned}\quad (23)$$

from the method described in Algorithm 1, the SMC multi-target state estimation can be easily obtained as

$$\widehat{X}_k = \left\{ \widehat{\mathbf{x}}_k^{(i)} \right\}_{i=1}^{\widehat{T}_k} \quad \text{with } \widehat{\mathbf{x}}_k^{(i)} = \sum_{l=1}^{L_k^{(i)}} \mathbf{x}_k^{(i,l)} \omega_k^{(i,l)}, \quad i = 1, \dots, \widehat{T}_k. \quad (24)$$

Note that the MCMC move step [26] can be introduced for increasing the particle variety after the resample step without affecting the validity of the SMC approximation.

5. GM-MM-CBMeMber Filter and Its EK and UK Extensions

An analytic solution to the MM-CBMeMber recursion for linear-Gaussian multiple maneuvering targets models is presented in this section. The resulting filter propagates the GM multi-Bernoulli density against time. Some certain assumptions about the linear-Gaussian multiple maneuvering targets models are firstly summarized below.

(A) The dynamic and measurement models for the augmented state of each maneuvering target have the form

$$\begin{aligned}f_{k|k-1}(\mathbf{x}_k, n_k | \mathbf{x}_{k-1}, n_{k-1}) &= \mathcal{N}(\mathbf{x}_k; F_k(n_k) \mathbf{x}_{k-1}, A_k(n_k) Q_k(n_k) (A_k(n_k))^T) \\ &\quad \times h_{k|k-1}(n_k | n_{k-1}), \\ g_k(\mathbf{z}_k | \mathbf{x}_k, n_k) &= \mathcal{N}(\mathbf{z}_k; H_k(n_k) \mathbf{x}_k, B_k(n_k) R_k(n_k) (B_k(n_k))^T),\end{aligned}\quad (25)$$

where $\mathcal{N}(\cdot; \mathbf{m}, P)$ denotes the density of Gaussian distribution with the mean \mathbf{m} and covariance P ; $F_k(n_k)$, $Q_k(n_k)$, and $A_k(n_k)$ are, respectively, the kinematical state transition, process noise covariance, and process noise coefficient matrixes conditioned on model n_k ; $H_k(n_k)$, $R_k(n_k)$, and $B_k(n_k)$ are, respectively, the observation, observation noise covariance, and observation noise coefficient matrixes conditioned on model n_k .

(B) The probabilities of maneuvering target survival and maneuvering target detection are independent of the kinematical state:

$$\begin{aligned}p_{S,k}(\mathbf{x}_{k-1}, n_{k-1}) &= p_{S,k}(n_{k-1}), \\ p_{D,k}(\mathbf{x}_k, n_k) &= p_{D,k}(n_k).\end{aligned}\quad (26)$$

(C) The birth model for the maneuvering targets is a multi-Bernoulli with parameter set $\{(\tilde{r}_{\Gamma,k}^{(i)}, \tilde{p}_{\Gamma,k}^{(i)}(\mathbf{x}_k, n_k))\}_{i=1}^{M_{\Gamma,k}}$, where $\tilde{p}_{\Gamma,k}^{(i)}(\mathbf{x}_k, n_k)$, $i = 1, \dots, M_{\Gamma,k}$, are GM of the form

$$\begin{aligned}\tilde{p}_{\Gamma,k}^{(i)}(\mathbf{x}_k, n_k) &= \tilde{p}_{\Gamma,k}^{(i)}(\mathbf{x}_k | n_k) h_{\Gamma,k}^{(i)}(n_k) \\ &= h_{\Gamma,k}^{(i)}(n_k) \sum_{j=1}^{J_{\Gamma,k}^{(i)}(n_k)} \tilde{\omega}_{\Gamma,k}^{(i,j)}(n_k) \\ &\quad \times \mathcal{N}(\mathbf{x}_k; \mathbf{m}_{\Gamma,k}^{(i,j)}(n_k), P_{\Gamma,k}^{(i,j)}(n_k)),\end{aligned}\quad (27)$$

where $h_{\Gamma,k}^{(i)}(n_k)$ is the distribution of model births and $\tilde{p}_{\Gamma,k}^{(i)}(\mathbf{x}_k | n_k)$ is the distribution of the birth kinematical state given model n_k . $\tilde{p}_{\Gamma,k}^{(i)}(\mathbf{x}_k | n_k)$ is GM of the form with the parameter set $\{\tilde{\omega}_{\Gamma,k}^{(i,j)}(n_k), \mathbf{m}_{\Gamma,k}^{(i,j)}(n_k), P_{\Gamma,k}^{(i,j)}(n_k)\}_{j=1}^{J_{\Gamma,k}^{(i)}(n_k)}$.

According to the above Assumptions A, B, and C, a closed form solution to the MM-CBMeMber recursion, namely, the GM-MM-CBMeMber filter, can be derived by applying the following two standard results for Gaussian functions:

$$\begin{aligned}\int \mathcal{N}(\mathbf{x}; F\mathbf{x}', Q) \mathcal{N}(\mathbf{x}'; \mathbf{m}, P) d\mathbf{x}' &= \mathcal{N}(\mathbf{x}; F\mathbf{m}, Q + FPF^T), \\ \mathcal{N}(\mathbf{z}; H\mathbf{x}, R) \mathcal{N}(\mathbf{x}; \mathbf{m}, P) &= \mathcal{N}(\mathbf{z}; H\mathbf{m}, R + HPH^T) \mathcal{N}(\mathbf{x}; \widehat{\mathbf{m}}, \widehat{P}),\end{aligned}\quad (28)$$

where

$$K = PH^T(HPH^T + R)^{-1},$$

$$\widehat{\mathbf{m}} = \mathbf{m} + K(\mathbf{z} - H\mathbf{m}), \quad (29)$$

$$\widehat{P} = (I - KH)P.$$

One cycle of the recursive GM-MM-CBMeMber algorithm can be described as follows.

(1) *The GM Mixing and Prediction Stage.* Suppose that at time $k-1$ the multi-Bernoulli posterior density $\bar{\pi}_{k-1}(Y_{k-1} | Z_{1:k-1}) = \{(\bar{r}_{k-1}^{(i)}, \bar{P}_{k-1}^{(i)}(\mathbf{x}_{k-1}, n_{k-1}))\}_{i=1}^{M_{k-1}}$ is given and each $\bar{P}_{k-1}^{(i)}(\mathbf{x}_{k-1}, n_{k-1})$, $i = 1, \dots, M_{k-1}$, is composed of GM of the form

$$\bar{P}_{k-1}^{(i)}(\mathbf{x}_{k-1}, n_{k-1})$$

$$= \sum_{j=1}^{J_{k-1}^{(i)}(n_{k-1})} \omega_{k-1}^{(i,j)}(n_{k-1}) \quad (30)$$

$$\times \mathcal{N}(\mathbf{x}_{k-1}; \mathbf{m}_{k-1}^{(i,j)}(n_{k-1}), P_{k-1}^{(i,j)}(n_{k-1})).$$

Then, the mixed and predicted multi-Bernoulli density $\bar{\pi}_{k|k-1}(Y_k | Z_{1:k-1}) = \{(\bar{r}_{P,k|k-1}^{(i)}, \bar{P}_{P,k|k-1}^{(i)}(\mathbf{x}_k, n_k))\}_{i=1}^{M_{k-1}} \cup \{(\bar{r}_{\Gamma,k}^{(i)}, \bar{P}_{\Gamma,k}^{(i)}(\mathbf{x}_k, n_k))\}_{i=1}^{M_{\Gamma,k}}$ can be computed as follows:

$$\bar{r}_{P,k|k-1}^{(i)} = \bar{r}_{k-1}^{(i)} \sum_{n_k} \sum_{n_{k-1}} \sum_{j=1}^{J_{k-1}^{(i)}(n_{k-1})} h_{k|k-1}(n_k | n_{k-1})$$

$$\times p_{S,k}(n_{k-1}) \bar{\omega}_{k-1}^{(i,j)}(n_{k-1}),$$

$$\bar{P}_{P,k|k-1}^{(i)}(\mathbf{x}_k, n_k) = \sum_{n_{k-1}} \sum_{j=1}^{J_{k-1}^{(i)}(n_{k-1})} \omega_{P,k|k-1}^{(i,j)}(n_k, n_{k-1})$$

$$\times \mathcal{N}(\mathbf{x}_k; \mathbf{m}_{P,k|k-1}^{(i,j)}(n_k, n_{k-1}), P_{P,k|k-1}^{(i,j)}(n_k, n_{k-1})),$$

$$\{(\bar{r}_{\Gamma,k}^{(i)}, \bar{P}_{\Gamma,k}^{(i)}(\mathbf{x}_k, n_k))\}_{i=1}^{M_{\Gamma,k}} = \text{given by the birth model (27)}, \quad (31)$$

where

$$\mathbf{m}_{P,k|k-1}^{(i,j)}(n_k, n_{k-1}) = F_k(n_k) \mathbf{m}_{k-1}^{(i,j)}(n_{k-1}),$$

$$P_{P,k|k-1}^{(i,j)}(n_k, n_{k-1}) = F_k(n_k) P_{k-1}^{(i,j)}(n_{k-1}) (F_k(n_k))^T$$

$$+ A_k(n_k) Q_k(n_k) (A_k(n_k))^T,$$

$$\omega_{P,k|k-1}^{(i,j)}(n_k, n_{k-1})$$

$$= (h_{k|k-1}(n_k | n_{k-1}) p_{S,k}(n_{k-1}) \bar{\omega}_{k-1}^{(i,j)}(n_{k-1}))$$

$$\times \left(\sum_{n_k} \sum_{n_{k-1}} \sum_{j=1}^{J_{k-1}^{(i)}(n_{k-1})} h_{k|k-1}(n_k | n_{k-1}) \right.$$

$$\left. \times p_{S,k}(n_{k-1}) \bar{\omega}_{k-1}^{(i,j)}(n_{k-1}) \right)^{-1}. \quad (32)$$

(2) *The GM Update Stage.* Suppose that at time k the mixed and predicted multi-Bernoulli density $\bar{\pi}_{k|k-1}(Y_k | Z_{1:k-1}) = \{(\bar{r}_{k|k-1}^{(i)}, \bar{P}_{k|k-1}^{(i)}(\mathbf{x}_k, n_k))\}_{i=1}^{M_{k|k-1}}$ is given and each $\bar{P}_{k|k-1}^{(i)}(\mathbf{x}_k, n_k)$, $i = 1, \dots, M_{k|k-1}$, is composed of GM of the form

$$\bar{P}_{k|k-1}^{(i)}(\mathbf{x}_k, n_k)$$

$$= \sum_{j=1}^{J_{k|k-1}^{(i)}(n_k)} \omega_{k|k-1}^{(i,j)}(n_k) \quad (33)$$

$$\times \mathcal{N}(\mathbf{x}_k; \mathbf{m}_{k|k-1}^{(i,j)}(n_k), P_{k|k-1}^{(i,j)}(n_k)).$$

Then, the multi-Bernoulli approximation of the updated density $\bar{\pi}_k(Y_k | Z_{1:k}) \approx \{(\bar{r}_{L,k}^{(i)}, \bar{P}_{L,k}^{(i)}(\mathbf{x}_k, n_k))\}_{i=1}^{M_{k|k-1}} \cup \{(\bar{r}_{U,k}(\mathbf{z}_k), \bar{P}_{U,k}(\mathbf{x}_k, n_k; \mathbf{z}_k))\}_{\mathbf{z}_k \in Z_k}$ can be computed as follows:

$$\bar{r}_{L,k}^{(i)} = \bar{r}_{k|k-1}^{(i)} \frac{1 - \sum_{n_k} \sum_{j=1}^{J_{k|k-1}^{(i)}(n_k)} \omega_{k|k-1}^{(i,j)}(n_k) p_{D,k}(n_k)}{1 - \bar{r}_{k|k-1}^{(i)} \sum_{n_k} \sum_{j=1}^{J_{k|k-1}^{(i)}(n_k)} \omega_{k|k-1}^{(i,j)}(n_k) p_{D,k}(n_k)},$$

$$\bar{r}_{U,k}(\mathbf{z}_k) = \left(\frac{\sum_{i=1}^{M_{k|k-1}} (1 - \bar{r}_{k|k-1}^{(i)}) \bar{r}_{k|k-1}^{(i)} \sum_{n_k} \sum_{j=1}^{J_{k|k-1}^{(i)}(n_k)} \omega_{k|k-1}^{(i,j)}(n_k) p_{D,k}(n_k) \bar{\mathcal{Q}}_k^{(i,j)}(n_k; \mathbf{z}_k)}{\left(1 - \bar{r}_{k|k-1}^{(i)} \sum_{n_k} \sum_{j=1}^{J_{k|k-1}^{(i)}(n_k)} \omega_{k|k-1}^{(i,j)}(n_k) p_{D,k}(n_k)\right)^2} \right)$$

$$\begin{aligned}
& \times \left(\kappa_k(\mathbf{z}_k) + \sum_{i=1}^{M_{k|k-1}} \frac{\bar{r}_{k|k-1}^{(i)} \sum_{n_k} \sum_{j=1}^{J_{k|k-1}^{(i)}(n_k)} \bar{\omega}_{k|k-1}^{(i,j)}(n_k) P_{D,k}(n_k) \mathcal{Q}_k^{(i,j)}(n_k; \mathbf{z}_k)}{1 - \bar{r}_{k|k-1}^{(i)} \sum_{n_k} \sum_{j=1}^{J_{k|k-1}^{(i)}(n_k)} \bar{\omega}_{k|k-1}^{(i,j)}(n_k) P_{D,k}(n_k)} \right)^{-1} \\
\bar{P}_{L,k}^{(i)}(\mathbf{x}_k, n_k) &= \frac{\sum_{j=1}^{J_{k|k-1}^{(i)}(n_k)} (1 - P_{D,k}(n_k)) \bar{\omega}_{k|k-1}^{(i,j)}(n_k) \mathcal{N}(\mathbf{x}_k; \mathbf{m}_{k|k-1}^{(i,j)}(n_k), P_{k|k-1}^{(i,j)}(n_k))}{1 - \sum_{n_k} \sum_{j=1}^{J_{k|k-1}^{(i)}(n_k)} \bar{\omega}_{k|k-1}^{(i,j)}(n_k) P_{D,k}(n_k)}, \\
\bar{P}_{U,k}^{(i)}(\mathbf{x}_k, n_k; \mathbf{z}_k) &= \sum_{i=1}^{M_{k|k-1}} \sum_{j=1}^{J_{k|k-1}^{(i)}(n_k)} \bar{\omega}_{U,k}^{(i,j)}(n_k; \mathbf{z}_k) \mathcal{N}(\mathbf{x}_k; \mathbf{m}_{U,k}^{(i,j)}(n_k; \mathbf{z}_k), P_{U,k}^{(i,j)}(n_k)),
\end{aligned} \tag{34}$$

where

$$\begin{aligned}
\mathcal{Q}_k^{(i,j)}(n_k; \mathbf{z}_k) &= \mathcal{N}(\mathbf{z}_k; H_k(n_k) \mathbf{m}_{k|k-1}^{(i,j)}(n_k), \\
& \quad B_k(n_k) R_k(n_k) (B_k(n_k))^T \\
& \quad + H_k(n_k) P_{k|k-1}^{(i,j)}(n_k) (H_k(n_k))^T) \\
\bar{\omega}_{U,k}^{(i,j)}(n_k; \mathbf{z}_k) &= \left(\frac{\bar{r}_{k|k-1}^{(i)}}{1 - \bar{r}_{k|k-1}^{(i)}} \bar{\omega}_{k|k-1}^{(i,j)}(n_k) P_{D,k}(n_k) \mathcal{Q}_k^{(i,j)}(n_k; \mathbf{z}_k) \right) \\
& \quad \times \left(\sum_{i=1}^{M_{k|k-1}} \sum_{n_k} \sum_{j=1}^{J_{k|k-1}^{(i)}(n_k)} \frac{\bar{r}_{k|k-1}^{(i)}}{1 - \bar{r}_{k|k-1}^{(i)}} \bar{\omega}_{k|k-1}^{(i,j)}(n_k) P_{D,k} \right. \\
& \quad \left. \times (n_k) \mathcal{Q}_k^{(i,j)}(n_k; \mathbf{z}_k) \right)^{-1} \tag{35}
\end{aligned}$$

$$\begin{aligned}
K_{U,k}^{(i,j)}(n_k) &= P_{k|k-1}^{(i,j)}(n_k) (H_k(n_k))^T \\
& \quad \times (H_k(n_k) P_{k|k-1}^{(i,j)}(n_k) (H_k(n_k))^T \\
& \quad + B_k(n_k) R_k(n_k) (B_k(n_k))^T)^{-1}, \\
\mathbf{m}_{U,k}^{(i,j)}(n_k; \mathbf{z}_k) &= \mathbf{m}_{k|k-1}^{(i,j)}(n_k) + K_{U,k}^{(i,j)}(n_k) \\
& \quad \times (\mathbf{z}_k - H_k(n_k) \mathbf{m}_{k|k-1}^{(i,j)}(n_k)),
\end{aligned}$$

$$P_{U,k}^{(i,j)}(n_k) = (I - K_{U,k}^{(i,j)}(n_k) H_k(n_k)) P_{k|k-1}^{(i,j)}(n_k).$$

(3) *The Pruning and Merging Stage.* It is the same as the pruning and merging stage of the GM-CBMeMber filter [16].

(4) *The GM Multitarget State Estimation.* Given the GM multi-Bernoulli posterior density

$$\begin{aligned}
\bar{\pi}_k(Y_k | Z_{1:k}) &= \left\{ (\bar{r}_k^{(i)}, \bar{p}_k^{(i)}(\mathbf{x}_k, n_k)) \right\}_{i=1}^{M_k} \text{ with} \\
\bar{p}_k^{(i)}(\mathbf{x}_k, n_k) &= \sum_{j=1}^{J_k^{(i)}(n_k)} \bar{\omega}_k^{(i,j)}(n_k) \mathcal{N}(\mathbf{x}_k; \mathbf{m}_k^{(i,j)}(n_k), P_k^{(i,j)}(n_k))
\end{aligned} \tag{36}$$

from the method described in Algorithm 1, the GM multitarget state estimation can be easily obtained as

$$\begin{aligned}
\widehat{X}_k &= \left\{ \widehat{\mathbf{x}}_k^{(i)} \right\}_{i=1}^{\widehat{T}_k} \text{ with } \widehat{\mathbf{x}}_k^{(i)} = \sum_{n_k} \sum_{j=1}^{J_k^{(i)}(n_k)} \bar{\omega}_k^{(i,j)}(n_k) \mathbf{m}_k^{(i,j)}(n_k), \\
& \quad i = 1, \dots, \widehat{T}_k.
\end{aligned} \tag{37}$$

Now turn to considering the extension of the GM-MM-CBMeMber filter to nonlinear dynamical and observation models using the EK filtering approximation. Assumptions B and C are still required, but the dynamic and observation processes can be relaxed to the nonlinear models

$$\begin{aligned}
\mathbf{x}_k &= a_k(\mathbf{x}_{k-1}, \mathbf{w}_k(n_k), n_k), \\
\mathbf{z}_k &= u_k(\mathbf{x}_k, \mathbf{v}_k(n_k), n_k),
\end{aligned} \tag{38}$$

where $a_k(\cdot, \cdot, n_k)$ and $u_k(\cdot, \cdot, n_k)$ are known model-dependent nonlinear functions, and $\mathbf{w}_k(n_k)$ and $\mathbf{v}_k(n_k)$ are model-dependent process and observation noise vectors of known statistics.

For the EK-GM-MM-CBMeMber filter, the closed form expressions for the mixing, prediction, and update of individual Gaussian components are approximated by replacing $F_k(n_k)$, $A_k(n_k)$, $H_k(n_k)$, $B_k(n_k)$ in the corresponding recursive equations (30)–(35) of the GM-MM-CBMeMber filter

with the corresponding local linearization of the nonlinear dynamical and observation models

$$\begin{aligned}
F_k^{\text{EK}}(n_k) &= \left. \frac{\partial a_k(\mathbf{x}_{k-1}, \mathbf{w}_k(n_k), n_k)}{\partial \mathbf{x}_{k-1}} \right|_{\substack{\mathbf{x}_{k-1} = \hat{\mathbf{x}}_{k-1} \\ \mathbf{w}_k(n_k) = \mathbf{0}}}, \\
A_k^{\text{EK}}(n_k) &= \left. \frac{\partial a_k(\mathbf{x}_{k-1}, \mathbf{w}_k(n_k), n_k)}{\partial \mathbf{w}_k(n_k)} \right|_{\substack{\mathbf{x}_{k-1} = \hat{\mathbf{x}}_{k-1} \\ \mathbf{w}_k(n_k) = \mathbf{0}}}, \\
H_k^{\text{EK}}(n_k) &= \left. \frac{\partial u_k(\mathbf{x}_k, \mathbf{v}_k(n_k), n_k)}{\partial \mathbf{x}_k} \right|_{\substack{\mathbf{x}_{k-1} = \hat{\mathbf{x}}_{k|k-1} \\ \mathbf{v}_k(n_k) = \mathbf{0}}}, \\
B_k^{\text{EK}}(n_k) &= \left. \frac{\partial u_k(\mathbf{x}_k, \mathbf{v}_k(n_k), n_k)}{\partial \mathbf{v}_k(n_k)} \right|_{\substack{\mathbf{x}_{k-1} = \hat{\mathbf{x}}_{k|k-1} \\ \mathbf{v}_k(n_k) = \mathbf{0}}}.
\end{aligned} \tag{39}$$

Note that the unscented Kalman version for the GM-MM-CBMeMber filter can be derived by approximating the mean and covariance of individual Gaussian components with a set of sigma points and the unscented transform [20]. Because of the space limitation, the details of the UK-GM-MM-CBMeMber filter are not presented here.

6. Simulations

6.1. Nonlinear Example Using SMC Implementations. In this nonlinear example, we evaluate the performance of the proposed MM-CBMeMber filter by benchmarking it against the single-model CBMeMber filters, the MM-PHD filter, and the MM-CPHD filter using the SMC implementations.

Consider a two-dimensional scenario with an unknown and time varying number of the maneuvering targets observed over the region $[-1000, 1000] \times [-1000, 1000]$ (m) for a period of $N = 50$ time steps. The sampling interval is $\Delta t = 1$ (s). Each of the targets may move at a nearly constant velocity or execute a coordinated turn in the surveillance period. Therefore, the model set designed for this example can be composed of a constant velocity (CV) model and a coordinated turn (CT) model with varying turn rate [27]. The target kinematical state is $\mathbf{x}_k = [x_k \ \dot{x}_k \ y_k \ \dot{y}_k \ \vartheta_k]^T$, where $[x_k \ y_k]^T$ and $[\dot{x}_k \ \dot{y}_k]^T$, respectively, represent the position and the velocity in x and y coordinates and ϑ_k represents the turn rate. For the turn rate ϑ_k , let the anticlockwise direction be positive and the clockwise direction be negative.

The model-dependent dynamics for the individual maneuvering target is given by the linear-Gaussian model

$$f_{k|k-1}(\mathbf{x}_k | \mathbf{x}_{k-1}, n_k) = \mathcal{N}(\mathbf{x}_k; F_k(n_k) \mathbf{x}_{k-1}, Q_k(n_k)). \tag{40}$$

Let $n_k = 1$ denote the CV model and $n_k = 2$ the CT model; then

$$\begin{aligned}
F_k(n_k = 1) &= \begin{bmatrix} F_{\text{CV}} & \\ & 0 \end{bmatrix}, \\
F_k(n_k = 2) &= \begin{bmatrix} F_{\text{CT}}(\vartheta_{k-1}) & \\ & 1 \end{bmatrix}, \\
Q_k(n_k = 1) &= \sigma_w^2(n_k = 1) \begin{bmatrix} Q & \\ & 0 \end{bmatrix}, \\
Q_k(n_k = 2) &= \begin{bmatrix} \sigma_{1,w}^2(n_k = 2) Q & \\ & \Delta t^2 \sigma_{2,w}^2(n_k = 2) \end{bmatrix}
\end{aligned} \tag{41}$$

with

$$\begin{aligned}
F_{\text{CV}} &= \begin{bmatrix} 1 & \Delta t & 0 & 0 \\ 0 & 1 & 0 & 0 \\ 0 & 0 & 1 & \Delta t \\ 0 & 0 & 0 & 1 \end{bmatrix}, \\
F_{\text{CT}}(\vartheta_{k-1}) &= \begin{bmatrix} 1 & \frac{\Delta t \sin \vartheta_{k-1}}{\vartheta_{k-1}} & 0 & -\frac{1 - \Delta t \cos \vartheta_{k-1}}{\vartheta_{k-1}} \\ 0 & \Delta t \cos \vartheta_{k-1} & 0 & -\Delta t \sin \vartheta_{k-1} \\ 0 & \frac{1 - \Delta t \cos \vartheta_{k-1}}{\vartheta_{k-1}} & 1 & \frac{\Delta t \sin \vartheta_{k-1}}{\vartheta_{k-1}} \\ 0 & \Delta t \sin \vartheta_{k-1} & 0 & \Delta t \cos \vartheta_{k-1} \end{bmatrix}, \\
Q &= \begin{bmatrix} \frac{\Delta t^4}{4} & \frac{\Delta t^3}{2} & 0 & 0 \\ \frac{\Delta t^3}{2} & \Delta t^2 & 0 & 0 \\ 0 & 0 & \frac{\Delta t^4}{4} & \frac{\Delta t^3}{2} \\ 0 & 0 & \frac{\Delta t^3}{2} & \Delta t^2 \end{bmatrix},
\end{aligned} \tag{42}$$

where $\sigma_w(n_k)$ is the level of the power spectral density of the process noise for model n_k . In this example, they are given by $\sigma_w(n_k = 1) = 0.1$ (m/s²), $\sigma_{1,w}(n_k = 2) = 0.2$ (m/s²), $\sigma_{2,w}(n_k = 2) = 1 \times 10^{-3}$ (rad/s²).

The Markovian model transition probability matrix is taken as

$$[n_{k|k-1}(n_k | n_{k-1})] = \begin{bmatrix} 0.8 & 0.2 \\ 0.2 & 0.8 \end{bmatrix}. \tag{43}$$

At time k , the range ρ_k and bearing φ_k measurements of the targets are generated by a sensor located at $[0 \ 0]^T$. The measurement noise is independent and identically distributed (IID) zero-mean Gaussian white noise with covariance matrix $R_k = \text{diag}(\sigma_\rho^2 \ \sigma_\varphi^2)$, where $\text{diag}(\cdot)$ denotes the diagonal matrix, and σ_ρ and σ_φ are, respectively, standard deviations (STDs) of the range and bearing measurements. In this example, they are taken as $\sigma_\rho = 10$ (m) and

$\sigma_\varphi = 0.01$ (rad). The single-measurement single-target likelihood density is

$$g_k(\mathbf{z}_k | \mathbf{y}_k) = \mathcal{N}\left(\mathbf{z}_k; \begin{bmatrix} \sqrt{x_k^2 + y_k^2} \\ \arctan \frac{y_k}{x_k} \end{bmatrix}, R_k\right). \quad (44)$$

The detection probability and the survival probability are, respectively, taken as $p_{D,k}(\mathbf{x}_k, n_k) = p_D = 0.95$ and $p_{S,k}(\mathbf{x}_{k-1}, n_{k-1}) = p_S = 0.95$ in this example.

The clutter is modeled as a Poisson RFS with the intensity $\kappa_k(\mathbf{z}_k) = \lambda_{c,k} f_{c,k}(\mathbf{z}_k)$. In this example, we take $\lambda_{c,k} = 20$ and $f_{c,k}(\cdot) = \mathcal{U}(\cdot)$, where $\mathcal{U}(\cdot)$ denotes the density of the uniform distribution over the observation region.

Figure 1 shows the true trajectories for the maneuvering targets and sensor location.

In Figure 1, “o” denotes the locations at which targets are born and “□” denotes the locations at which targets die. Target 1 is born at 1 s and dies at 30 s. It first moves at a nearly constant velocity from the first second to the 15th second and then executes a coordinated turn in the anticlockwise direction from the 16th second to the 30th second. Target 2 is born at 1 s and dies at 35 s. It first executes a coordinated turn in the anticlockwise direction from the first second to the 20th second and then moves at a nearly constant velocity from the 21st second to the 35th second. Target 3 is born at 10 s and dies at 42 s. It first executes a coordinated turn in the anticlockwise direction from the 10th second to the 30th second and then moves at a nearly constant velocity from the 31st second to the 42nd second. Target 4 is born at 20 s and dies at 50 s. It first moves at a nearly constant velocity from the 20th second to the 30th second and then executes a coordinated turn in the clockwise direction from the 31st second to the 50th second. The motions of the targets are summarized in Table 1.

The birth process is a multi-Bernoulli RFS with density $\pi_{\Gamma,k}(Y_k) = \{(r_{\Gamma,k}^{(i)} p_{\Gamma,k}^{(i)}(\mathbf{x}_k, n_k))\}_{i=1}^3$, where $r_{\Gamma,k}^{(1)} = 0.04$, $r_{\Gamma,k}^{(2)} = r_{\Gamma,k}^{(3)} = 0.02$, $p_{\Gamma,k}^{(i)}(\mathbf{x}_k, n_k) = h_{\Gamma,k}^{(i)}(n_k) \mathcal{N}(\mathbf{x}_k; \mathbf{m}_{\Gamma,k}^{(i)}, P_{\Gamma,k}^{(i)})$ with

$$\begin{aligned} \mathbf{m}_{\Gamma,k}^{(1)} &= [-600 \ 0 \ 800 \ 0 \ 0]^T, \\ \mathbf{m}_{\Gamma,k}^{(2)} &= [-650 \ 0 \ -800 \ 0 \ 0]^T, \\ \mathbf{m}_{\Gamma,k}^{(3)} &= [400 \ 0 \ -400 \ 0 \ 0]^T, \end{aligned} \quad (45)$$

$$P_{\Gamma,k}^{(1)} = P_{\Gamma,k}^{(2)} = P_{\Gamma,k}^{(3)} = \text{diag}(400 \ 400 \ 400 \ 400 \ 0.01)$$

and the distribution of the model births

$$[h_{\Gamma,k}^{(i)}(n_k)] = [0.5 \ 0.5]. \quad (46)$$

For the purpose of comparison, we estimate the number and states of the maneuvering targets using the proposed SMC-MM-CBMeMber filter, the CV model SMC-CBMeMber filter, the CT model SMC-CBMeMber filter, the SMC-MM-PHD filter, and the SMC-MM-CPHD filter, respectively. At each time step in the SMC implementations of the CBMeMber-based filters, a maximum of $L_{\max} = 1000$ and minimum of $L_{\min} = 300$ particles per hypothesized

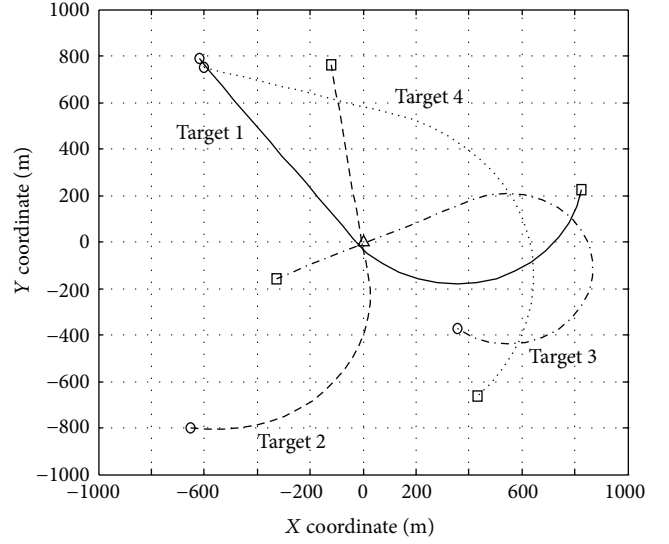


FIGURE 1: The true trajectories for the maneuvering targets and sensor location.

TABLE 1: The motions of the targets.

	Born time	Die time	CV motion	CT motion
Target 1	1 s	30 s	1 s–15 s	16 s–30 s, anticlockwise
Target 2	1 s	35 s	21 s–35 s	1 s–20 s, anticlockwise
Target 3	10 s	42 s	31 s–42 s	10 s–30 s, anticlockwise
Target 4	20 s	50 s	20 s–30 s	31 s–50 s, clockwise

track are imposed, and pruning of hypothesized tracks is performed with a threshold of $\tilde{r}_{\text{threshold}} = 0.001$. At each time step in the SMC implementations of the PHD-based filters, 1000 particles are used to represent one target and K -means method [14] is used to cluster the resampled particles to extract the multitarget states. The proposal densities $\alpha_k^{(i)}(n_k | n_{k-1})$, $\beta_k^{(i)}(n_k)$, $q_k^{(i)}(\mathbf{x}_k | \mathbf{x}_{k-1}, n_k, Z_k)$, and $b_k^{(i)}(\mathbf{x}_k | n_k, Z_k)$ in (16) and (18) are, respectively, taken as $h_{k|k-1}(n_k | n_{k-1})$, $h_{\Gamma,k}^{(i)}(n_k)$, $f_{k|k-1}(\mathbf{x}_k | \mathbf{x}_{k-1}, n_k)$ and $\mathcal{N}(\mathbf{x}_k; \mathbf{m}_{\Gamma,k}^{(i)}, P_{\Gamma,k}^{(i)})$. We now conduct 500 Monte Carlo (MC) simulation experiments on the same clutter intensity and target trajectories, but with independently generated clutter and target-generated measurements in each trial.

The MC averages of the mean and STD of the cardinality distribution for the five methods at each time step are shown along with the true target number in Figure 2, respectively.

Figures 2(a)–2(e) demonstrate that the target number estimates from the SMC-MM-PHD, SMC-MM-CPHD, and SMC-MM-CBMeMber filters converge to the ground truth, whereas the CV model SMC-CBMeMber and CT model SMC-CBMeMber filters produce significant bias in estimating the target number. This is because the SMC-MM-PHD, SMC-MM-CPHD, and SMC-MM-CBMeMber filters can effectively capture the model switching property of the maneuvering targets, so their performance is significantly better than that of the two single-model SMC-CBMeMber

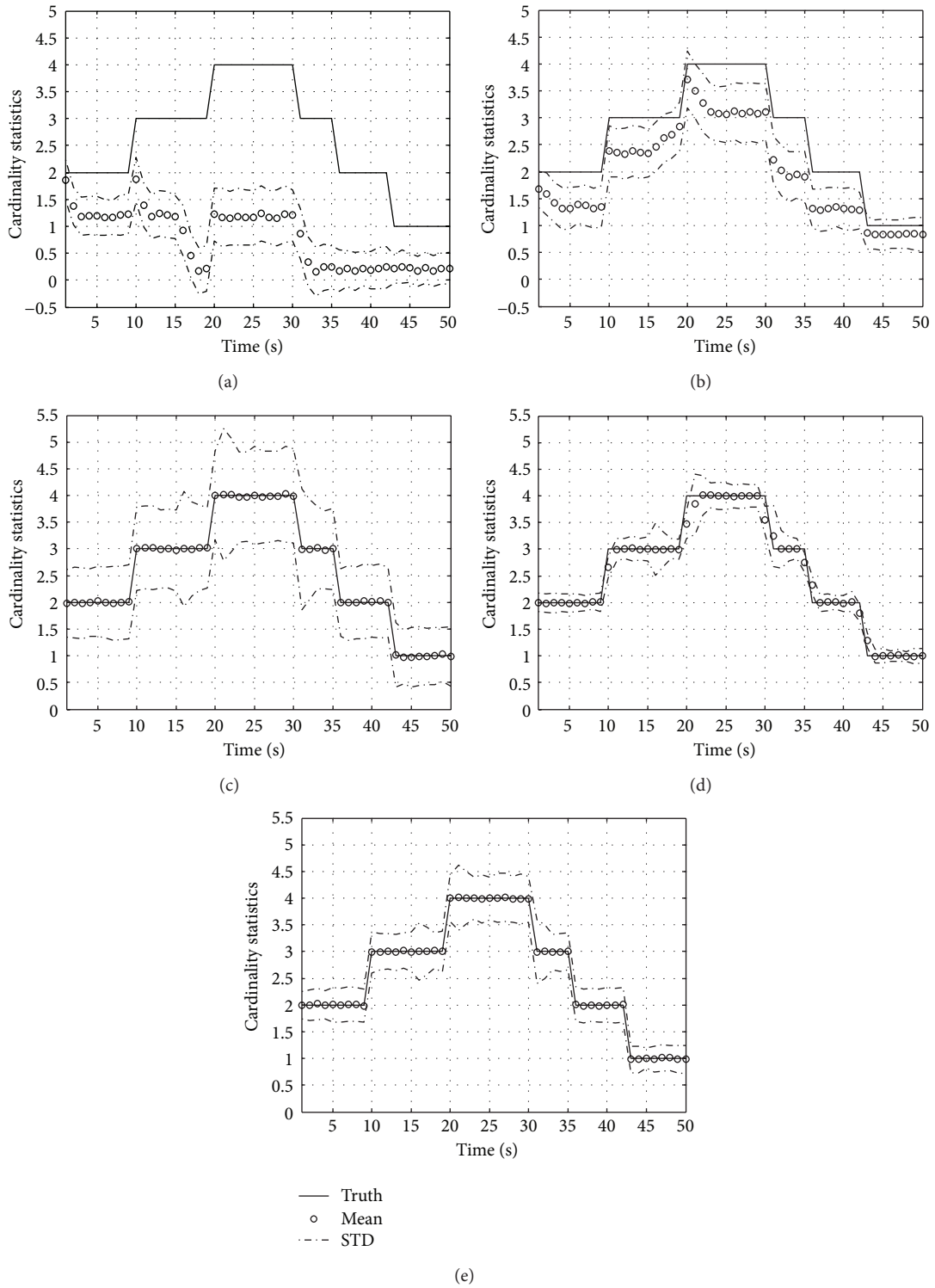


FIGURE 2: The 500 MC run averages of cardinality statistics versus time for the (a) CV model SMC-CBMeMber filter, (b) CT model SMC-CBMeMber filter, (c) SMC-MM-PHD filter, (d) SMC-MM-CPHD filter, and (e) SMC-MM-CBMeMber filter.

filters, which show poor adaptation to target maneuvers and yield larger estimation errors.

Moreover, as plotted in Figures 2(c)–2(e), the STD of the cardinality distribution from the SMC-MM-CBMeMber filter is lower than that of the SMC-MM-PHD filter, but larger than that of SMC-MM-CPHD filter. In addition, the STDs of the cardinality distributions from the three MM-based filters increase in different degrees at the instances when the maneuver occurs (i.e., 16 (s), 21 (s), and 31 (s)). The STD plots of the SMC-MM-PHD and SMC-MM-CPHD filters seem to fluctuate more obviously than the SMC-MM-CBMeMber filter. This phenomenon indicates that the performance of the SMC-MM-CBMeMber filter may be more stable and robust at the maneuver instances than that of the SMC-MM-PHD and SMC-MM-CPHD filters.

The optimal subpattern assignment (OSPA) metric [28], which can jointly capture differences in cardinality and individual elements between two finite sets, is used to evaluate the performance of the five methods. Given the actual and estimated multitarget state sets $X_k = \{\mathbf{x}_k^{(i)}\}_{i=1}^{T_k}$ and $\widehat{X}_k = \{\widehat{\mathbf{x}}_k^{(i)}\}_{i=1}^{\widehat{T}_k}$, the OSPA metric of order $p = 2$ with cut-off c between the two sets is defined by

$$\begin{aligned} \text{OSPA}_{2,k}^{(c)}(X_k, \widehat{X}_k) &= \left(\frac{1}{\widehat{T}_k} \left(\min_{\pi \in \Pi_{\widehat{T}_k}} \sum_{i=1}^{T_k} \min(c, \|\mathbf{x}_k^{(i)} - \widehat{\mathbf{x}}_k^{(\pi(i))}\|_2)^2 \right. \right. \\ &\quad \left. \left. + c^2 (\widehat{T}_k - T_k) \right) \right)^{1/2} \end{aligned} \quad (47)$$

if $T_k \leq \widehat{T}_k$ and $\text{OSPA}_{2,k}^{(c)}(X_k, \widehat{X}_k) = \text{OSPA}_{2,k}^{(c)}(\widehat{X}_k, X_k)$ if $T_k > \widehat{T}_k$. $\Pi_{\widehat{T}_k}$ denotes the set of permutations on $\{1, 2, \dots, \widehat{T}_k\}$. $\|\cdot\|_2$ denotes the 2-norm. In this example, we take $c = 100$ (m).

The MC averages of the OSPA metric for the target position estimates, derived by the five methods, are shown in Figure 3.

The OSPA metric is composed of two components each separately accounting for “localization” and “cardinality” errors. This results in high peaks in OSPA metric at the instances where the estimated number is incorrect. Figure 3 shows that (1) both the single-model SMC-CBMeMber filters perform significantly worse than the other MM-based filters because of the large cardinality errors produced by the two filters as seen in Figures 2(a) and 2(b); (2) although the SMC-MM-CPHD filter can estimate the target number most accurately, the OSPA metric of the SMC-MM-CBMeMber filter is smaller than that of the SMC-MM-CPHD filter, which is in turn smaller than that of the SMC-MM-PHD filter. This phenomenon indicates that the SMC-MM-CBMeMber filter outperforms the SMC-MM-CPHD (and hence SMC-MM-PHD) filter in jointly estimating the multitarget number and states. A reason for this is that the additional errors could be introduced in the clustering processes of the SMC-MM-PHD and SMC-MM-CPHD filters to extract state estimates from the particle population; (3) the OSPA plots of

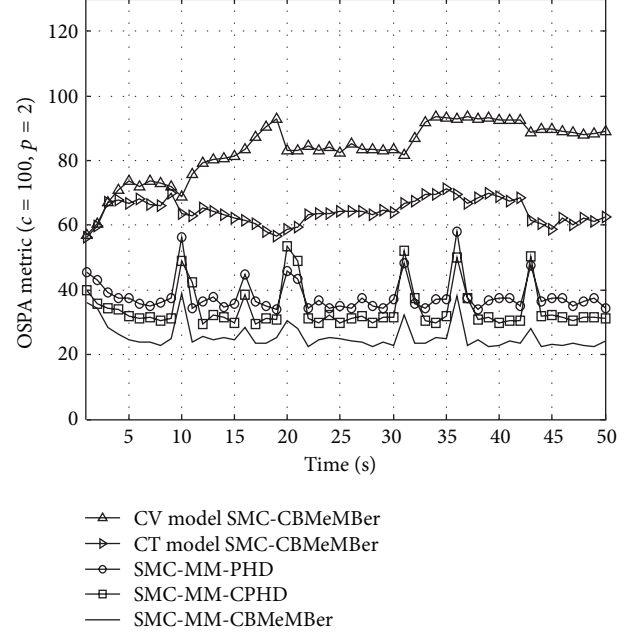


FIGURE 3: The 500 MC run averages of OSPA against time.

the three MM-based filters in Figure 3 fluctuate against time due to the varying target number, the target maneuvers, and clutter. However, increase of the OSPA from the SMC-MM-CBMeMber filter seems to be smallest at the maneuver instances (i.e., 16 (s), 21 (s), and 31 (s)) among the three MM-based methods. This phenomenon also indicates that the performance of the SMC-MM-CBMeMber filter may be more stable and robust at the maneuver instances than that of the SMC-MM-PHD and SMC-MM-CPHD filters.

For comparing the overall performance of the three MM-based filters, the 500 MC trial averages of the OSPA distance (time-averaged over the duration of the scenario) for the three MM-based filters are shown in Table 2 against the clutter rate from $\lambda_{c,k} = 20$ to $\lambda_{c,k} = 100$. The result of time-averaging can be viewed as a broad indication of filter performance, although the average is likely to be scenario dependent.

Table 2 shows that the OSPA distances of the three MM-based filters increase with higher $\lambda_{c,k}$. It reflects that the performance of the three MM-based algorithms degrades by different degrees as the $\lambda_{c,k}$ increases. Among the three MM-based algorithms, the SMC-MM-PHD filter always works the worst. The SMC-MM-CBMeMber filter outperforms the SMC-MM-CPHD filter when $\lambda_{c,k}$ is relatively lower ($\lambda_{c,k} \leq 60$). However, as the $\lambda_{c,k}$ increases, the OSPA distance of SMC-MM-CBMeMber filter increases more rapidly than that of the SMC-MM-CPHD filter. Therefore, as $\lambda_{c,k}$ continues to increase until it reaches $\lambda_{c,k} = 80$, the OSPA distance of SMC-MM-CBMeMber filter is very close to that of the SMC-MM-CPHD filter. When $\lambda_{c,k}$ is relatively higher (i.e., $\lambda_{c,k} = 80$), the SMC-MM-CPHD filter outperforms the SMC-MM-CBMeMber filter. A possible reason for this is that, compared

TABLE 2: Time-averaged OSPA distance (m) in various $\lambda_{c,k}$.

	$\lambda_{c,k} = 20$	$\lambda_{c,k} = 40$	$\lambda_{c,k} = 60$	$\lambda_{c,k} = 80$	$\lambda_{c,k} = 100$
SMC-MM-PHD filter	38.3	48.2	60.5	74.3	88.1
SMC-MM-CPHD filter	32.8	35.9	39.4	43.4	47.8
SMC-MM-CBMeMber filter	25.6	31.3	37.4	43.2	48.9

with the SMC-MM-CBMeMber filter, the advantage of the target number estimate for the SMC-MM-CPHD filter is more obvious as the $\lambda_{c,k}$ increases and it finally leads that the OSPA distance of the SMC-MM-CPHD filter is smaller than that of the SMC-MM-CBMeMber filter when $\lambda_{c,k}$ is relatively higher (i.e., $\lambda_{c,k} = 80$).

6.2. Linear-Gaussian Example Using GM Implementations. In this linear-Gaussian example, we evaluate the performance of the proposed MM-CBMeMber filter by benchmarking it against the single-model CBMeMber filters, the MM-PHD filter, and the MM-CPHD filter using the GM implementations.

The simulation scenario and true trajectories for the maneuvering targets are the same as those of Example 1. The target kinematical state now turns into $\mathbf{x}_k = [x_k \ \dot{x}_k \ y_k \ \dot{y}_k]^T$. The model set for this example is designed as follows. Model $n_k = 1$ is a CV model with linear-Gaussian dynamics given by $\mathcal{N}(\mathbf{x}_k; F_{CV}\mathbf{x}_{k-1}, \sigma_{CV,w}^2 Q)$; models $n_k = 2, 3, 4, 5$ are, respectively, CT models with turn rates of $\vartheta = \pi/30, -\pi/30, \pi/20, \pi/15$ (rad/s) with linear-Gaussian dynamics given by $\mathcal{N}(\mathbf{x}_k; F_{CT}(\vartheta)\mathbf{x}_{k-1}, \sigma_{CT,w}^2 Q)$. In this example, $\sigma_{CV,w}$ and $\sigma_{CT,w}$ are given by $\sigma_{CV,w} = 0.1$ (m/s²), $\sigma_{CT,w} = 0.2$ (m/s²).

The Markovian model transition probability matrix now turns into

$$[h_{k|k-1}(n_k | n_{k-1})] = \begin{bmatrix} 0.6 & 0.1 & 0.1 & 0.1 & 0.1 \\ 0.1 & 0.6 & 0.1 & 0.1 & 0.1 \\ 0.1 & 0.1 & 0.6 & 0.1 & 0.1 \\ 0.1 & 0.1 & 0.1 & 0.6 & 0.1 \\ 0.1 & 0.1 & 0.1 & 0.1 & 0.6 \end{bmatrix}. \quad (48)$$

The x -position and y -position measurements $\mathbf{z}_k = [x_k \ y_k]^T$ of the maneuvering targets are generated by the linear-Gaussian single-measurement single-target likelihood density given by $\mathcal{N}(\mathbf{z}_k; H_k \mathbf{x}_k, R_k)$ with

$$H_k = \begin{bmatrix} 1 & 0 & 0 & 0 \\ 0 & 0 & 1 & 0 \end{bmatrix} \quad (49)$$

and $R_k = \text{diag}(\sigma_x^2 \ \sigma_y^2)$. In this example, they are taken as $\sigma_x = \sigma_y = 8$ (m), and the kinematical state independent survival and detection probabilities are taken as $p_{D,k}(n_k) = p_D = 0.95$ and $p_{S,k}(n_{k-1}) = p_S = 0.95$.

The experiment settings of the clutter and birth model are also the same as those of Example 1 except that the $\mathbf{m}_{\Gamma,k}^{(i)}, P_{\Gamma,k}^{(i)}$, $i = 1, 2, 3$, and $[h_{\Gamma,k}^{(i)}(n_k)]$ turn into

$$\begin{aligned} \mathbf{m}_{\Gamma,k}^{(1)} &= [-600 \ 0 \ 800 \ 0]^T, \\ \mathbf{m}_{\Gamma,k}^{(2)} &= [-650 \ 0 \ -800 \ 0]^T, \\ \mathbf{m}_{\Gamma,k}^{(3)} &= [400 \ 0 \ -400 \ 0]^T, \end{aligned} \quad (50)$$

$$P_{\Gamma,k}^{(1)} = P_{\Gamma,k}^{(2)} = P_{\Gamma,k}^{(3)} = \text{diag}(400 \ 400 \ 400 \ 400),$$

$$[h_{\Gamma,k}^{(i)}(n_k)] = [0.2 \ 0.2 \ 0.2 \ 0.2 \ 0.2].$$

For the purpose of comparison, we estimate the number and states of the maneuvering targets using the proposed GM-MM-CBMeMber filter, the CV model GM-CBMeMber filter, the CT model GM-CBMeMber filter with turn rate of $\vartheta = \pi/20$ (rad/s), (this turn rate seems to be most suitable for the scenario among the above four turn rates), the GM-MM-PHD filter, and the GM-MM-CPHD filter, respectively. At each time step in the GM implementations of the CBMeMber-based filters, pruning of hypothesized tracks is performed with a threshold of $\tilde{r}_{\text{threshold}} = 0.001$. In addition, the pruning and merging of Gaussian components are performed for each hypothesized track using a weight threshold of 10^{-5} , a merging threshold of 4 (m), and a maximum of $J_{\text{max}} = 100$ components, which are also used in the GM implementations of the PHD-based filters.

The MC averages of the mean and STD of the cardinality distribution for the five methods at each time step are shown along with the true target number in Figure 4, respectively.

Similar to the SMC implementations, Figures 4(a)–4(e) demonstrate that the GM implementations of the three MM-based filters are unbiased in the target number estimates, whereas the GM implementations of the two single-model GM-CBMeMber filters are significantly biased. Moreover, the GM-MM-CBMeMber filter has a lower STD of the estimated cardinality than the GM-MM-PHD filter but has a larger STD than the GM-MM-CPHD filter. Again, The STD plots of the GM-MM-PHD and GM-MM-CPHD filters seem to fluctuate more obviously than the GM-MM-CBMeMber filter at the maneuver instances (i.e., 16 (s), 21 (s), and 31 (s)).

The MC averages of the OSPA metric for the target position estimates, derived by the five methods, are shown in Figure 5.

In contrast to the SMC case, Figure 5 shows that (1) the rather poor performance of the two single-model GM-CBMeMber filters can be expected as the direct results of their significant cardinality bias as seen in Figures 4(a) and

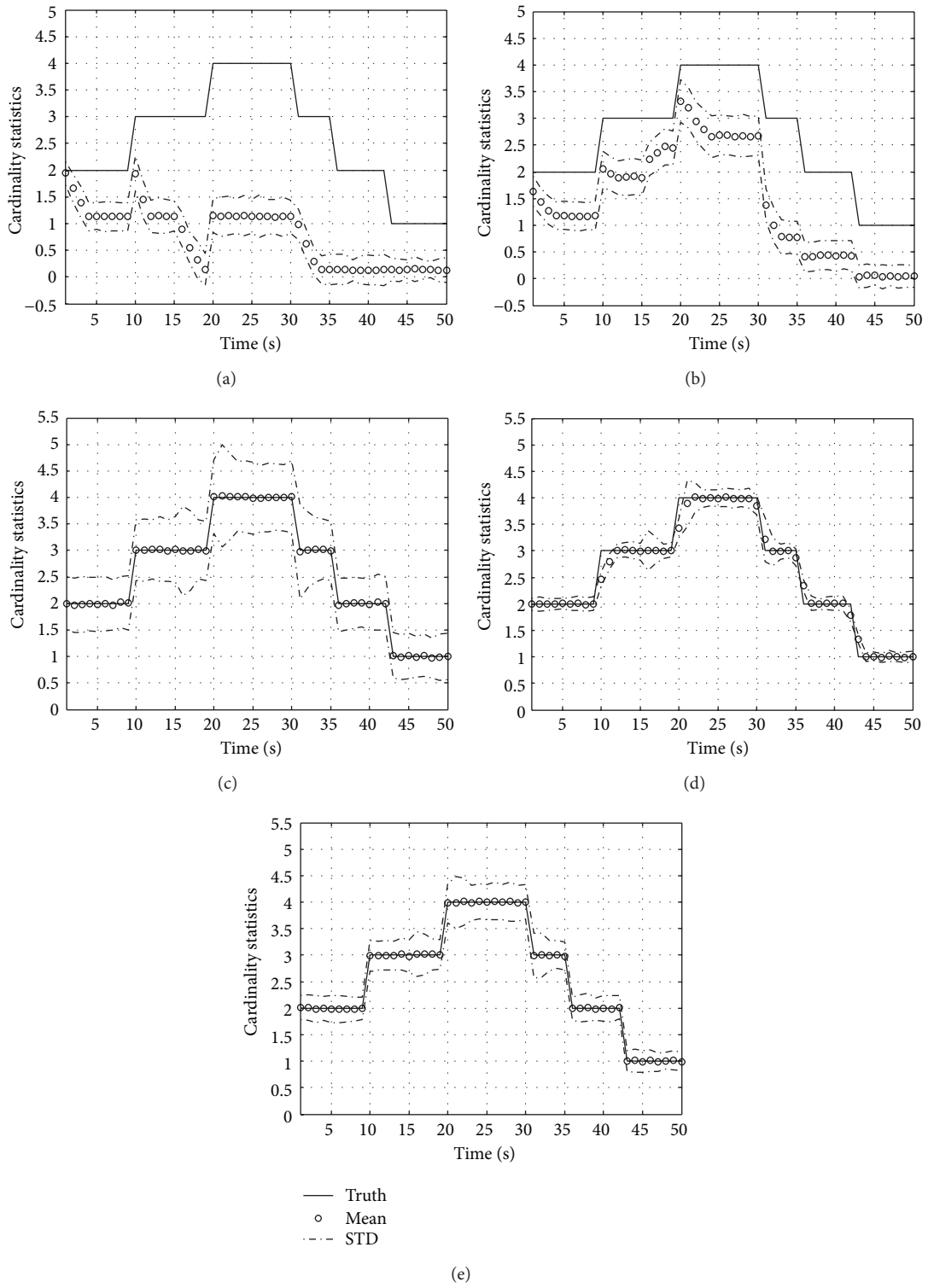


FIGURE 4: The 500 MC run averages of cardinality statistics versus time for the (a) CV model GM-CBMeMber filter, (b) CT model GM-CBMeMber filter, (c) GM-MM-PHD filter, (d) GM-MM-CPHD filter, and (e) GM-MM-CBMeMber filter.

TABLE 3: Time-averaged OSPA distance (m) in various $\lambda_{c,k}$.

	$\lambda_{c,k} = 20$	$\lambda_{c,k} = 40$	$\lambda_{c,k} = 60$	$\lambda_{c,k} = 80$	$\lambda_{c,k} = 100$
GM-MM-PHD filter	22.8	28.2	34.5	40.9	47.1
GM-MM-CPHD filter	20.0	24.8	30.3	36.1	41.9
GM-MM-CBMeMber filter	22.6	27.7	34.1	40.6	46.7

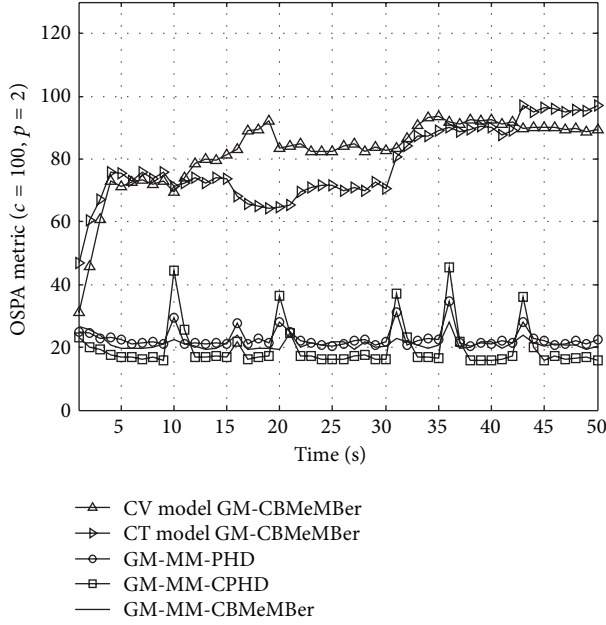


FIGURE 5: The 500 MC run averages of OSPA against time.

4(b); (2) the OSPA metric of the GM-MM-CBMeMber filter is similar to that of the GM-MM-PHD filter but is larger than that of the GM-MM-CPHD filter. This is because that, like the MM-CBMeMber filter, the GM implementations of the MM-PHD and MM-CPHD filters also allow state estimates to be extracted from the posterior intensity in a much more efficient and reliable manner than particle clustering in the SMC-based approach. As a result, the GM-MM-CPHD filter, which has the lowest STD of the estimated cardinality, performs best among the three MM-based filters. Although the GM-MM-CBMeMber filter has a lower STD of the estimated cardinality than the GM-MM-PHD filter, the performance of the two filters is similar. A reason for this is that the GM-MM-PHD filter may have more of an advantage than the GM-MM-CBMeMber filter in the relatively high signal to noise ratio (SNR) of this scenario.

Although the GM-MM-CPHD filter outperforms the proposed GM-MM-CBMeMber filter, it can be only used in the linear-Gaussian condition. In the nonlinear non-Gaussian conditions, both the MM-CPHD filter and MM-CBMeMber filter must be implemented by the SMC method. In this case, the GM-MM-CBMeMber filter outperforms the GM-MM-CPHD filter significantly, which is shown in Section 6.1.

The 500 MC trial averages of the OSPA distance (time-averaged over the duration of the scenario) for the three

MM-based filters are shown in Table 3 against the clutter rate from $\lambda_{c,k} = 20$ to $\lambda_{c,k} = 100$.

Similar to the SMC implementations, Table 3 shows that the OSPA distances of the GM implementations of the three MM-based filters increase with higher $\lambda_{c,k}$. However, in various $\lambda_{c,k}$, the GM-MM-CPHD filter always has the best performance among the three MM-based algorithms, and the GM-MM-CBMeMber filter has the similar performance with the GM-MM-PHD filter.

7. Conclusions and Future Work

An MM-CBMeMber filter, which is a multiple-model extension to the CBMeMber filter, is proposed for tracking multiple maneuvering targets in clutter. The SMC and GM implementations of the proposed filter are, respectively, presented for generic models and for linear-Gaussian models. Then, the EK and UK filtering approximations for the GM-MM-CBMeMber filter in nonlinear condition are described briefly. Simulation results show that (1) the proposed MM-CBMeMber filter significantly outperforms the single-model CBMeMber filters in tracking multiple maneuvering targets; (2) under relatively low clutter density, the SMC-MM-CBMeMber filter outperforms the SMC-MM-PHD and SMC-MM-CPHD filters; (3) the performance of the GM-MM-CBMeMber filter is similar to that of the GM-MM-PHD filter and hence is inferior to that of GM-MM-CPHD filter.

The future work is focused on the following three aspects. First, the track labeling problem in the proposed approach needs to be considered. Second, practical data need to be used for the performance evaluation of the proposed approaches. Third, the multiple-sensor versions of the CBMeMber and MM-CBMeMber filters need to be proposed for improving the performance of the single-sensor CBMeMber and MM-CBMeMber filters.

Acknowledgments

This research work was supported by the National Key Fundamental Research & Development Programs (973) of China (2013CB329405), Foundation for Innovative Research Groups of the National Natural Science Foundation of China (61221063), Natural Science Foundation of China (61203221, 61004087), Ph.D. Programs Foundation of Ministry of Education of China (20100201120036), China Postdoctoral Science Foundation (2011M501442, 20100481338), and Fundamental Research Funds for the Central University.

References

- [1] I. R. Goodman, R. P. S. Mahler, and H. T. Nguyen, *Mathematics of Data Fusion*, Kluwer Academic, Norwood, Mass, USA, 1997.
- [2] R. Mahler, *Statistical Multisource Multitarget Information Fusion*, Artech House, Norwood, Mass, USA, 2007.
- [3] R. Mahler, "Multi-target Bayes filtering via first-order multi-target moments," *IEEE Transactions on Aerospace and Electronic Systems*, vol. 39, no. 4, pp. 1152–1178, 2003.
- [4] R. Mahler, "PHD filters of higher order in target number," *IEEE Transactions on Aerospace and Electronic Systems*, vol. 43, no. 4, pp. 1523–1543, 2007.
- [5] T. Zajic and R. Mahler, "A particle-systems implementation of the PHD multitarget tracking filter," in *The International Society for Optical Engineering*, vol. 5096 of *Proceedings of SPIE*, pp. 291–299, April 2003.
- [6] H. Sidenbladh, "Multi-target particle filtering for the probability hypothesis density," in *Proceedings of the 6th International Conference on Information Fusion*, pp. 800–806, Cairns, Australia, 2003.
- [7] B.-N. Vo, S. Singh, and A. Doucet, "Sequential Monte Carlo methods for multi-target filtering with random finite sets," *IEEE Transactions on Aerospace and Electronic Systems*, vol. 41, no. 4, pp. 1224–1245, 2005.
- [8] B.-N. Vo and W.-K. Ma, "The Gaussian mixture probability hypothesis density filter," *IEEE Transactions on Signal Processing*, vol. 54, no. 11, pp. 4091–4104, 2006.
- [9] B.-T. Vo, B.-N. Vo, and A. Cantoni, "Analytic implementations of the cardinalized probability hypothesis density filter," *IEEE Transactions on Signal Processing*, vol. 55, no. 7, pp. 3553–3567, 2007.
- [10] H. Zhang, Z. Jing, and S. Hu, "Gaussian mixture CPHD filter with gating technique," *Signal Processing*, vol. 89, no. 8, pp. 1521–1530, 2009.
- [11] D. Clark, I. T. Ruiz, Y. Petillot, and J. Bell, "Particle PHD filter multiple target tracking in sonar image," *IEEE Transactions on Aerospace and Electronic Systems*, vol. 43, no. 1, pp. 409–416, 2007.
- [12] E. Maggio, M. Taj, and A. Cavallaro, "Efficient multitarget visual tracking using random finite sets," *IEEE Transactions on Circuits and Systems for Video Technology*, vol. 18, no. 8, pp. 1016–1027, 2008.
- [13] F. Lian, C. Han, W. Liu, J. Liu, and J. Sun, "Unified cardinalized probability hypothesis density filters for extended targets and unresolved targets," *Signal Processing*, vol. 92, no. 7, pp. 1729–1744, 2012.
- [14] D. E. Clark and J. Bell, "Multi-target state estimation and track continuity for the particle PHD filter," *IEEE Transactions on Aerospace and Electronic Systems*, vol. 43, no. 4, pp. 1441–1453, 2007.
- [15] W. Liu, C. Han, F. Lian, and H. Zhu, "Multitarget state extraction for the PHD filter using MCMC approach," *IEEE Transactions on Aerospace and Electronic Systems*, vol. 46, no. 2, pp. 864–883, 2010.
- [16] B.-T. Vo, B.-N. Vo, and A. Cantoni, "The cardinality balanced multi-target multi-Bernoulli filter and its implementations," *IEEE Transactions on Signal Processing*, vol. 57, no. 2, pp. 409–423, 2009.
- [17] R. Hoseinnezhad, B.-N. Vo, B.-T. Vo, and D. Suter, "Bayesian integration of audio and visual information for multi-target tracking using a CB-member filter," in *Proceedings of the 36th IEEE International Conference on Acoustics, Speech, and Signal Processing (ICASSP '11)*, pp. 2300–2303, Prague, Czech Republic, May 2011.
- [18] X. R. Li and V. P. Jilkov, "Survey of maneuvering target tracking—part V: multiple-model methods," *IEEE Transactions on Aerospace and Electronic Systems*, vol. 41, no. 4, pp. 1255–1321, 2005.
- [19] W. Mei, G. Shan, and C. Wang, "Practical development of the second-order extended Kalman filter for very long range radar tracking," *Signal Processing*, vol. 91, no. 5, pp. 1240–1248, 2011.
- [20] S. Sadhu, S. Mondal, M. Srinivasan, and T. K. Ghoshal, "Sigma point Kalman filter for bearing only tracking," *Signal Processing*, vol. 86, no. 12, pp. 3769–3777, 2006.
- [21] K. Punithakumar, T. Kirubarajan, and A. Sinha, "Multiple-model probability hypothesis density filter for tracking maneuvering targets," *IEEE Transactions on Aerospace and Electronic Systems*, vol. 44, no. 1, pp. 87–98, 2008.
- [22] S. A. Pasha, B.-N. Vo, H. D. Tuan, and W.-K. Ma, "A Gaussian mixture PHD filter for jump Markov system models," *IEEE Transactions on Aerospace and Electronic Systems*, vol. 45, no. 3, pp. 919–936, 2009.
- [23] C. Ouyang, H.-B. Ji, and Z.-Q. Guo, "Extensions of the SMC-PHD filters for jump Markov systems," *Signal Processing*, vol. 92, no. 6, pp. 1422–1430, 2012.
- [24] W. Li and Y. Jia, "Gaussian mixture PHD filter for jump Markov models based on best-fitting Gaussian approximation," *Signal Processing*, vol. 91, no. 4, pp. 1036–1042, 2011.
- [25] R. Georgescu and P. Willett, "The multiple model CPHD tracker," *IEEE Transactions on Signal Processing*, vol. 60, no. 4, pp. 1741–1751, 2012.
- [26] A. Doucet, N. J. Gordon, and V. Krishnamurthy, "Particle filters for state estimation of jump Markov linear systems," *IEEE Transactions on Signal Processing*, vol. 49, no. 3, pp. 613–624, 2001.
- [27] X. R. Li and V. P. Jilkov, "A survey of maneuvering target tracking: dynamic models," in *Signal and Data Processing of Small Targets*, vol. 4048 of *Proceedings of SPIE*, pp. 212–235, Orlando, Fla, USA, April 2000.
- [28] D. Schuhmacher, B.-T. Vo, and B.-N. Vo, "A consistent metric for performance evaluation of multi-object filters," *IEEE Transactions on Signal Processing*, vol. 56, no. 8, pp. 3447–3457, 2008.